Chapter 16
Activated Carbon Injection for In-Situ Remediation of Petroleum Hydrocarbons

Scott Noland and Edward Winner

Abstract In-situ remediation of petroleum hydrocarbons (PHCs) using activated carbon (AC) is an emerging technology intended to enhance sorption and biodegradation mechanisms in soil and groundwater systems. The combination of pore types, source material, activation process, and grind of a particular AC influences its efficacy in subsurface remediation. When high-energy injection techniques are employed, installation of carbon-based injectate (CBI) slurries can be conducted in practically any geological setting, from sandy aquifers to low-permeability zones and weathered or fractured rock. Following an adequate CBI installation throughout the target treatment zone or as a permeable reactive barrier, dissolved PHC concentrations are typically observed to rapidly decrease. After a new equilibrium is formed, PHC concentrations typically decrease over time due to the biodegradation. PHC biodegradation, in association with the CBIs, is indicated by the presence of appropriate microbial communities found to grow on AC and is supported by multiple lines of evidence. Further research is encouraged to optimize the biodegradation and regeneration processes of CBI products for in-situ remediation of PHCs.

Keywords Activated carbon · Biodegradation · Carbon-based injectate · Direct-push injection · Permeable reactive barrier

16.1 Introduction

In-situ remediation of petroleum hydrocarbons (PHCs) using activated carbon (AC) is an emerging technology enhancing sorption and often treatment via biodegradation of soil and groundwater contaminants.

S. Noland (✉) · E. Winner
Remediation Products Inc., 6390 Joyce Drive, Golden, CO 80403, USA
e-mail: scott@remediationproducts.com

E. Winner
e-mail: ed@remediationproducts.com

J. García-Rincón et al. (eds.), *Advances in the Characterisation and Remediation of Sites Contaminated with Petroleum Hydrocarbons*, Environmental Contamination Remediation and Management, https://doi.org/10.1007/978-3-031-34447-3_16

Installation of carbon-based injectates (CBI) can be done using direct-push technology (DPT) or other methods in practically any geological setting, from sandy aquifers to low-permeability zones and weathered or fractured rock when high-energy injection techniques are employed. Many variables must be determined before going to the field, including injection point grid spacing (both areal and vertical) across the target treatment zone, injection tips, pressure and injection flow rate, the mass of AC product to be injected at each depth and location, and top-down versus bottom-up injection technique.

It is well known that most adsorption of organic compounds occurs in the microporous structure of AC and that these pores are much smaller than bacteria capable of degrading these contaminants. Compelling evidence exists that compounds residing in micropores are assimilated by bacteria. AC has a number of characteristics that support microbial life and healthy growth including formation of microbial clusters and reduction of contaminant toxicity toward the microorganism. Specific microbes often found at PHC impacted sites are described along with lines of evidence that can be developed for demonstrating biodegradation is occurring. Use of compound-specific isotope analysis (CSIA) as a means of proving biodegradation of specific contaminants is discussed along with case study examples. See Chap. 11 for more information on the use of CSIA in petroleum-contaminated sites.

The concept of biological regeneration of AC is developed. This concept is of pivotal importance because effective regeneration of carbon creates a dynamic system that will continue to perform over long periods of time and not be limited by adsorption capacity. The chapter ends with a discussion of future research needs to address fundamental questions such as whether co-injection of bacterial consortia significantly improves performance and how indigenous microbes interact under bioaugmentation. In addition, we explore applications involving light non-aqueous phase liquid (LNAPL) from the perspective of adsorption capacity, toxicity, and biological response and limitations associated with low concentrations such as those often encountered with the fuel additive methyl tert-butyl ether (MTBE).

16.2 Characteristics of Activated Carbon

AC is composed of plates of hexagonal carbon rings. Many of the hexagonal rings are cleaved such that they are orientated out of the primary plane relative to most of the carbon rings. These ring cleavages also allow other rings structures such as pentagons and heptagons. These carbon rings, when viewed at a larger scale, form curved sheets, bowels, and ribbons (Harris et al. 2008). The interaction of these structures forms walls, resulting in cavities and passages commonly referred to as pores. Pores are both the passages into deeper sections of AC particles and the volume above surfaces upon which adsorbed compounds bind.

AC has a large hydrophobic surface that binds molecules through van der Waals forces and other physicochemical bonds related to the presence of different pore types within its structure. The pore structure is thus the primary physical characterization

of AC. The pores are classified into three major groups based on pore diameter. The largest pores are macropores (pore diameter > 50 nm), followed by mesopores (pore diameter from 2 to 50 nm). These pores are important pathways for the diffusion of molecules into the carbon structure and to the micropores. The micropores (pore diameter < 2 nm) are where most of the adsorption occurs because in the micropores the gaps between the carbon plates are only a few molecular diameters. The binding forces, termed London forces, are weak and only influence a range of 1–5 molecular diameters from the carbon plates (Greenbank 1993). For perspective on the size of the AC pores, the smallest bacteria are about 200 nm, while the typical petroleum-degrading bacterium would be a rod around 600 by 400 nm (Weiss 1995).

The combination of pore types, source material, activation process, and grind of a particular AC influence its efficacy in subsurface remediation. AC derives from carbon source materials that have been chemically treated and/or heat-treated in a controlled atmosphere to drive off volatiles and increase porosity (Menendez Diaz 2006). AC source materials are carbon-rich substances such as bituminous coal, coconut shell, rice husks, and wood. The choice of material from which the AC is made significantly affects the adsorption character of the AC (Zango 2020). For example, despite being rich in binding pores (micropores), coconut-based AC exhibits slower kinetic adsorption performance due to having relatively fewer transport pores (McNamara 2018). The activation technique or process also affects the adsorptive characteristics of the resulting AC (Menendez Diaz 2006; Lillo-Ródenas 2005). Thus, oxygen-containing groups on the AC generally increase adsorption of compounds like toluene, and such groups are increased by acid modification but decreased with alkali modification (Ma 2019). On the other hand, alkali modification improves o-xylene adsorption to AC (Li 2011). The specific source material, activation technique, and post-activation processing combine to make many types of AC, each of which has unique adsorptive characteristics (Cheremisinoff 1978; Menendez Diaz 2006).

AC is available in a range of grinds or mesh sizes, but the products used for in-situ remediation are typically categorized as granular, powered, or colloidal (Fan 2017). As a broad statement, the smaller the grind, the faster the initial adsorption and subsequent desorption because the micropores increase as a percentage of all pores but are closer to the particle surface (Liang 2007; Piai 2019). For practical purposes in application to hydrocarbon remediation, the rate of adsorption across the various grinds is so fast that the grind is not selected based on adsorption rate.

Since the introduction of AC-based technologies for in-situ remediation of PHCs in early 2002, several products have been developed as shown in Table 16.1. Colloidal products are designed to be injected under low-energy conditions, while powdered AC (PAC) and granular AC (GAC) products are typically injected under pressure.

Table 16.1 Commercially available AC-based products for in-situ PHC remediation

Product	Property	PHC degradation pathway	Manufacturer
BOS 200®	PAC mixed with nutrients, electron acceptors, and facultative bacteria	Aerobic and anaerobic bioaugmentation	RPI
BOS 200+®	BOS 200® enhanced for application to LNAPL sites	Aerobic and anaerobic bioaugmentation	RPI
Plume Stop®	Colloidal AC suspension with an organic stabilizer	Anaerobic biodegradation via biostimulation	Regenesis
Petrofix®	Colloidal AC suspension with electron acceptors including sulfate and/or nitrate	Aerobic and anaerobic biodegradation	Regenesis
COGAC®	GAC or PAC mixed with calcium peroxide and sodium persulfate	Chemical oxidation. Aerobic and anaerobic biostimulation	Remington technologies
FluxSorb™	Colloidal carbon product	Aerobic and anaerobic biodegradation	Cascade

16.3 Application of Activated Carbon to In-Situ Petroleum Remediation

Compared to many conventional technologies for in-situ remediation, the performance of AC-based systems is relatively unaffected by certain subsurface conditions. For example, the adsorption characteristics of AC are the same in seawater and freshwater despite the different geochemical conditions. AC is inert, so it does not typically react with the geology to mobilize ions or metals. In addition, AC can be installed in a wide range of geological settings, from sandy aquifers to low-permeability zones and weathered or fractured rock when high-energy techniques are employed. Injecting AC into the subsurface may thus result in contaminant concentration reduction over a broad range of subsurface conditions, particularly when adequate contact between the AC and the contaminant is established and if a contaminant destruction mechanism such as biodegradation is simultaneously promoted. The objective of all injection designs should be to achieve contact between contaminant and CBI and match dosing of CBI to the distribution of contaminant mass.

16.3.1 Installation

AC amendments can be delivered to the subsurface via injection across the target treatment zone or as a permeable reactive barrier (PRB). A water-based carrier fluid is typically used to suspend AC of a wide particle size range prior to injection. Large

AC particle suspensions (5–50 μm mean diameter size) are typically referred to as slurries, while colloidal suspensions aided by dispersants are typically achieved using smaller AC particles (2–10 μm). Once injected, AC is expected to affix to the formation.

Colloidal carbon suspensions can be injected with low-pressure, low-flow techniques where the pump pressure is adjusted to ensure fracture pressures of the formation are not exceeded. Amendment distribution typically follows naturally existing fluid pathways when low-pressure injection is employed. The rate at which a colloidal carbon both agglomerates and affixes to the formation depends on the medium of suspension or dispersant employed (Haupt 2019). Slurries of AC are typically jetted into the subsurface, with the AC material being expected to settle out three to five meters from the injection points. High-pressure injection is commonly used to facilitate emplacement of CBIs in heterogeneous systems by creating secondary porosity within a region localized around the injection point.

Multiple techniques exist to deliver CBIs into the subsurface, including gravity feed, DPT, modified augers, soil mixing, and trenching. Straddle-packers are employed to allow pressurizing and isolating an injection interval in open hole bedrock installations or in other formations where DPT cannot penetrate the ground. Alternatively, boreholes can be grouted with bentonite clay (uniformly hydrated, distributed, and cured to avoid injection fluid to migrate up the well, i.e., daylighting).

Gravity feed relies on the hydraulic head of the injectate typically stored in a tank to create flow into a fixed well and through its screen (or through a hollow drill rod) into the subsurface. This approach is commended for its low cost and simplicity, yet it is not generally or effective. Gravity feed techniques are useful for large volume solution injections and require high-permeability formations. Injected fluids are preferably low in viscosity, and suspensions should be well dispersed and with small mean particle size that can flow past screens, well completion sands, and formation particles. This technique is typically considered inadequate of CBI particles settle out of suspension more quickly than they can be distributed. Preferential pathways observed during gravity feed techniques may also limit the capability of uniformly distributing CBI across a contaminated interval.

The most common CBI installation technique uses DPT with pump-supported injection with pump-supported injection to emplace the CBI in discrete intervals within the subsurface. Injection with DPT consists of driving hollow drill rods into the ground through hammering. The rod is configured with an injection tip. Once the tip is at a desired depth, an injection head is attached on surface and pumps force solutions, slurries, and gels through the rod and into the subsurface.

Injection pressures and flow rates primarily depend on nature of the geology and injection fluid. Low-pressure injection and high-pressure injection techniques can be employed to install CBIs. In high-permeability tills, either method can be effective (McGregor 2020). In low-permeability geologies (hydraulic conductivity below 10^{-5} m/s), it is difficult for low-pressure methods to achieve sufficient distribution and adequate contact with contaminants. High-pressure techniques are superior (Christiansen 2010).

Note that pressure gauges on most (if not all) injection pump systems are located near the pump discharge. At any given flow rate, the pressure at this location is mostly an indication of the pressure drop across the pipes, fittings, hoses, and tooling. Additional calculations or the use of a downhole pressure gauge are required to measure the pressure at the formation (i.e., at depth).

16.3.2 Injection Technique and Spacing

The relative difficulty of distributing AC in the subsurface results in implementation designs using low-volume injections across a high-density injection point grid within the target treatment zone or PRB. These points are laid out horizontally in a triangular grid along the direction of contaminant transport. The spacing between injection points should be adjusted based on geological setting, project goals, and costs. The distance between horizontally placed injection points is informed by experience. Efforts to control distribution out beyond three to six meters are rarely successful in overburden materials because moving closer to the surface correlates with a decreasing weight of the overburden and a corresponding decrease in resistence to flow.

Regarding the vertical spacing between discrete injection depths, a similar installation practice consists of alternating injection depths within the treatment zone on adjacent points. This injection depth "staggering" approach helps ensure that all targeted depth intervals receive CBI. Experience has shown that in low-permeability materials, injections can be completed every 0.5–0.6 m in depth. In high-permeability materials, the ideal spacing is around 1 m, and high-energy injection techniques are required to achieve good distribution of injectate in this case.

Regarding the injection technique, bottom-up injections should be avoided when fine-grained sediments are present. Imagine completing the first injection at depth, then as the injection rod is withdrawn to the next targeted zone, the borehole below the rod remains open. In this type of profile, it takes more pressure to open a fracture than it does to propagate the deeper one, and injectate will simply flow into the first injection location. Bottom-up injections are effective in heaving sand. In general, injections should be completed in a top–down manner so that as injections are completed, the rod is advanced, and it tends to seal off the previous location and prevent injectate cross-circuiting.

16.4 Patterns of AC Distribution

After injection, the CBI will ultimately follow the path of least resistance. As discussed in Chaps. 1, 4, 7, and 8 among others, subsurface properties can vary widely over small scales so it is challenging to predict where CBIs may travel when

forced into the formation. Through high-pressure injection (jetting and fracture generation), some control over placement of CBI can be exerted within a region localized around the injection point. However, energy quickly dissipates, and further outward movement of injectate is again relegated to low resistance pathways. In sedimentary environments, small gradations in particle size distributions can represent low resistance pathways and channel flow of injectate.

CBIs is intensely black in color and can be recognized in most cores collected after injection. As illustrated in Fig. 16.1, PAC injected under pressure is commonly found in the form of thin horizontal seams and sometimes as angular or vertical features following the path of least resistance. This is also depicted in Fig. 16.2, where CBI follow subtle differences in sediment texture. CBI injection flow paths are often found to preferentially follow strata interfaces or high-permeability pathways.

Injection of slurries into sands is more challenging than injecting solutions because the suspended solids tend to be filtered from the injectate. Water readily moves through saturated sands, leaving suspended solids localized in a small region around the point of injection if low-energy injection is employed. High-energy injection

Fig. 16.1 Excavation post-CBI emplacement in the vadose zone demonstrates significant horizontal distribution. The CBI contained PAC. Note the horizontal carbon sheet above the bucket mark traced by a yellow line (dashed). The carbon sheet was ~1.2 m across. A shallower horizontal sheet is traced by an orange line (solid). Two angular carbon sheets having more vertical character are marked by red lines (dotted)

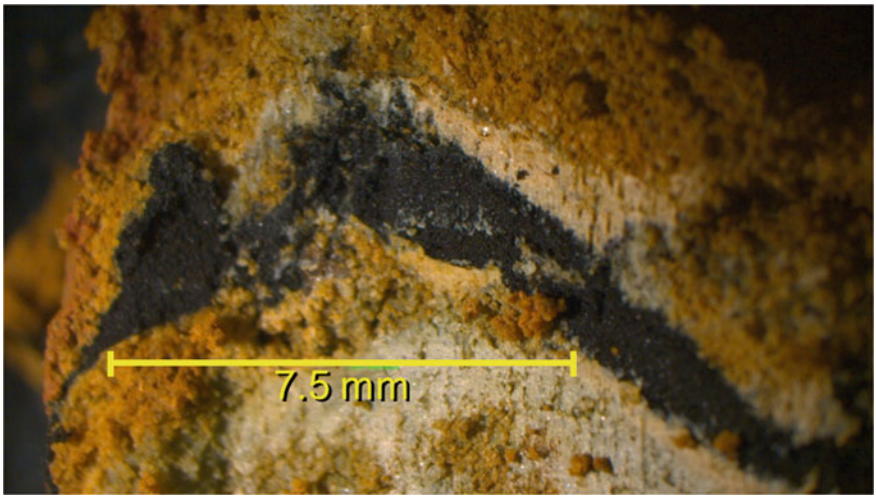

Fig. 16.2 PAC intercalated between materials exhibiting subtle texture variations

Fig. 16.3 Distribution of AC throughout aquifer sands after high-energy injection. The sleeve is a standard 3.6-cm diameter tube

techniques can overcome this difficulty as depicted in Fig. 16.3, where a slurry of granular AC was jetted into the aquifer sands at an exit velocity of over 60 m/s.

In summary, high pressure and flow can be employed to force slurries out from the point of injection and emplace it in both high- and low-permeability formations. On the contrary, low-flow and low-pressure (low energy) injection techniques will not distribute most CBI in clay lenses or other low-permeability zones. One strength of colloidal AC-based injectate is that vary uniform distributions in sands, and other high-permeability materials can be achieved under low-flow and low-pressure conditions.

16.5 Amount of Carbon Injected

The amount of carbon to be installed at a particular site will depend on the remedial goals established for that site. Figure 16.4 is an idealized model intended to help the reader understand the amount of carbon that needs to be injected to address a

mass of contamination. Think of a mixing tank containing some volume (V) of water with of water with a dissolved contaminant at an initial concentration (Co). Adding and mixing a mass of AC (W) results in an equilibrium dissolved concentration (Ce) with a certain mass of contaminant adsorbed to the carbon. The concentration of contaminant sorbed in the AC is denoted Sc. In this system, a simple mass balance can be written as follows (Eq. 16.1):

$$\mathrm{CoV} = \mathrm{CeV} + \mathrm{WSc} \tag{16.1}$$

The left side of Eq. (16.1) is the mass of the contaminant in the vessel (CoV). The first term on the right is the mass of contaminant dissolved in water at equilibrium (CeV). The last term is the mass of contaminant adsorbed in carbon (WSc). Therefore, increasing the amount of carbon increases the contaminant adsorbed to the carbon and decreases the contaminant in the aqueous phase at equilibrium.

In order for the above mass balance to be useful, a relationship (isotherm) between dissolved phase equilibrium concentration and the concentration of contaminant adsorbed in the AC is needed. A variety of different isotherm equations have been proposed, some have a theoretical foundation, and some are empirical in nature. Commonly, the Langmuir or Freundlich isotherms are used to model adsorption behavior. The Freundlich isotherm is often applied to adsorption of organic compounds onto AC and is written as follows (Eq. 16.2):

$$\mathrm{Sc} = k\mathrm{Ce}^{1/n} \tag{16.2}$$

A plot of Ce versus Sc in log–log space yields a linear-plot whose slope is ($1/n$) and intercept is (k). Substituting into the mass balance for Sc yields the following equation (Eq. 16.3):

$$\mathrm{CoV} = \mathrm{CeV} + \mathrm{WkCe}^{1/n}. \tag{16.3}$$

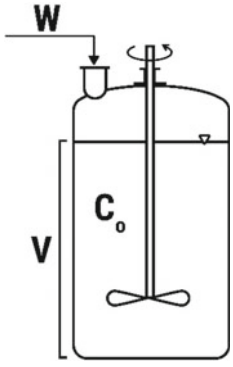

Fig. 16.4 Idealized model to understand how much carbon may need to be injected consisting of a mixing tank containing some volume (V) of water with a dissolved contaminant at an initial concentration (Co) where some mass of AC (W) is added and mixed

For example, if we have 10 ppm toluene in groundwater and our target is to reduce the concentration to 0.5 ppm, we can look up the Freundlich parameters (Dobbs 1980), $k = 26.1$ and $1/n = 0.44$. Alternatively, isotherms are often available from product vendors. Assuming an average porosity of 30%, there will be 300 L of groundwater per cubic meter of saturated formation. The only unknown is W, which can be calculated as in the equation below (Eq. 16.4):

$$W = 300(10 - 0.5)/26.1(0.5)^{0.44} = 148\,\text{g AC per cubic meter of saturated formation.} \tag{16.4}$$

This model is simplistic and does not reflect the complexities found in the subsurface. It is impossible to obtain complete mixing, and, usually, there are multiple contaminants competing for adsorption to AC. In the field, PHC impacted sites may be some of the most complex in that contamination consists of a multitude of adsorbates that interact very differently with AC that could require the development of isotherms specific to the PHC products found on a site. A simplification arises when concentration of absorbable species is low. In this case, each adsorbate equilibrium will be unaffected by the presence of other components. This presumption would likely apply at locations in the plume where only dissolved phase exists but not within or near an LNAPL source zone.

Typically, the practical experience of CBI vendors and installers suggests application of an engineering factor of safety (EFS) to estimated mass dosing from isotherm calculations. While efforts have been made to develop EFS systematically, the factors remain a matter of experience and commonly vary from two to tenfold the mass dose estimated based on isotherms. When very small amounts of AC are apparently needed, this is when the highest EFS are indicated. A more extensive AC loading increases the probability of contact between AC and a contaminant when the contaminant is present in low concentration.

The previous discussion regarding calculation of injection mass dosing applies to plume-wide treatment. With permeable reactive barriers (PRBs), one needs to consider the contaminant mass flux across and through the barrier, the design life of the barrier, and contaminant degradation during transition through the barrier. PRBs constructed with CBI can be thought of as a conventional carbon bed. In a conventional carbon bed, contaminant mass is adsorbed by the carbon as it enters the bed. Adsorption continues until the adsorption capacity of the carbon is approached, and the contaminant then travels a bit further into the bed. As this process continues, a narrow zone forms that slowly moves through the bed. This zone is called the mass transfer zone. The barrier design is based on the amount of carbon adsorption needed to meet the contaminant concentration goals on the downgradient side of the barrier for a defined time. Many references, e.g., (Thomas 1998; Ruthven 1984), describe how flow-through AC beds are designed. In a CBI PRB, biodegradation can contribute to increase the PRB operational lifespan. Biodegradation effects could also be accounted for during the design of the PRB to optimize the amount of carbon needed.

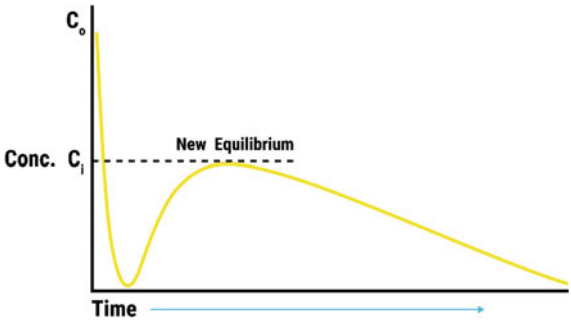

Fig. 16.5 Idealized general response in terms of contaminant concentration in groundwater after CBI installation

16.6 General Response to Installation of AC into a Contaminated Aquifer

After AC-based injectate for passive in-situ remediation of soil and groundwater was introduced to the industry (Noland 2002), initial expectations of some practitioners were that dissolved phase contaminants would simply disappear due to adsorption, and contaminated sites would clean up overnight. This expectation has been tempered over time as the complexities of subsurface environments and inefficiencies associated with CBI installation have come to be appreciated.

Figure 16.5 depicts an idealized general response in terms of contaminant concentration in groundwater after CBI installation. Dissolved contaminants are rapidly adsorbed, and the transient concentration reduction is often better than predicted based on design. This is because an equilibrium initially existed between the dissolved and sorbed mass of contaminant. The injection of AC disrupts this equilibrium as the rate of adsorption of contaminant from groundwater outpaces the rate of contaminant desorption from the formation. As contaminant desorbs from the formation into groundwater, adsorption continues, and the interplay between adsorption capacity of the AC and the contaminant mass flux from the formation results in rising concentrations in the aqueous phase until a new equilibrium is established (Ci on Fig. 16.5).

The magnitude of Ci and the time required for a new equilibrium to be established is a function of the contaminant mass initially present in the aquifer, the distribution of AC within the formation, and the stratigraphy. If the target treatment zone resides in a high-permeability environment, the time to achieve a new equilibrium will be short, often within a few weeks. If the aquifer sediments consist of silt or clay, the time required may span months. What is often incorrectly called “rebound” is a predictable partitioning of contaminant mass between the groundwater, the aquifer solids, and the AC as the system approaches a new equilibrium.

Presuming no significant contaminant mass is present that would cause overloading of the carbon and assuming robust biological activity is operating to degrade contaminants, a general decline from Ci should be observed. Given a general decline,

a semilog plot of concentration over time should result in a straight line with a negative slope that will be related to the rate of contaminant degradation.

16.6.1 Effects Related to Contaminant Mass

The most important variable affecting the response to injection of AC into the aquifer is the amount of contaminant mass present. At locations far removed from a source area and where the contaminant mass sorbed to the formation is insignificant, observed post-injection concentration perturbances are slight if they occur.

In contrast, the other extreme is represented by significant non-aqueous phase liquid (NAPL) hydrocarbon in the formation. This condition is common in source areas, and it is unlikely that enough CBI can be injected to absorb the NAPL altogether. After injection of CBI, experience has shown that a short-term drop in dissolved phase concentration is often observed; however, recontamination of groundwater due to continued contact with NAPL may overcome the adsorption capacity of the CBI, and a return to original conditions is predictable.

The above-described static state should not be interpreted as a deterrent to using CBI to treat NAPL. Instead of employing a design based simply on adsorption capacity, the design should be based on the surface area of the injected AC. NAPL mass removal rates are a function of the total amount of AC injected due to the available surface area of the AC that supports degradation. Regardless of adsorption, more surface area correlates to increased biodegradation. In this manner, AC is like a catalyst. This allows one to predict the time required to eliminate NAPL and see the subsequent decline in groundwater concentration. This is very similar to measurement of carbon dioxide generation at NAPL sites to estimate the average mass removal rate and then use that rate to predict performance over time.

16.6.2 Competitive Desorption

There is a widely held belief within the environmental industry that organic compounds, once adsorbed to AC, are stabilized for, perhaps, centuries. An article published in 2015 stated: “organic compounds are sorbed to AC so strongly that it is almost certain that the contamination will be stable and unavailable for leaching for at least 50–100 years” (Fox 2015). The reality is that the adsorption of organic compounds is a reversible process controlled by the heat (enthalpy) of adsorption (Kolasinski 2019). This feature has significant consequences.

AC will efficiently remove contaminants from groundwater and soil until the adsorption capacity is reached. Refined petroleum, whether gasoline, diesel, or other fuels, contains many different organic compounds. AC interacts with all these compounds differently as heats of adsorption are specific to each compound, and there will be competition for available absorption sites on the AC. In addition, naturally

occurring organic matter (NOM) also must be considered. Some dissolved organic compounds (NOM) are present in all groundwater, and they typically have high heats of adsorption and will also compete for adsorption sites.

When AC is first injected, adsorption sites within the carbon are unoccupied, and there is a vast space for compounds to bind. It does not matter if some compounds bind more energetically to AC than others; initially, there is room. As the space begins to fill up, those compounds with higher heats of adsorption tend to displace those having lower heats of adsorption. Now, those compounds with low heats of adsorption begin to desorb from the carbon into solution, while other compounds with high heats of adsorption continue to be adsorbed. This process is called "roll-over" within the AC industry, i.e., displacement of compounds having lower heats of adsorption.

Important examples of this are benzene and 1,2-dichloroethane. It is common for benzene concentration to be a site risk driver. Benzene has a relatively low heat of adsorption and can be displaced from AC by any number of common contaminants, including xylene, naphthalene, and NOM. To mitigate bleeding of contaminants from the AC, robust degradation mechanisms or pathways must be present to effectively remove and degrade adsorbed compounds from the carbon. Ideally, the rate at which compounds are degraded should effectively maintain unoccupied adsorption sites on the AC. This facilitates continuing adsorption of new contaminants without displacing those already bound to the AC. The most common means for accomplishing this with PHCs is biological degradation. The AC is biologically regenerated as bound contaminants are degraded. This mechanism will be discussed in the next section.

The proposed degradation mechanisms should be carefully evaluated whenever CBI technology is considered. Any application of CBI to contaminants where no viable degradation mechanism is known should be conscientiously weighted because the installed CBI may become a new source in the future. The clearest example of this is the use of AC at sites impacted by per and polyfluoroalkyl substances (PFAS), known as "forever chemicals" in the vernacular. A complete CBI remediation system must be supported by a treatment mechanism. Biodegradation is the preferred mechanism for most CBIs on the market intended for remediation of PHCs.

16.6.3 Adsorption by Activated Carbon

Literally every municipality in the USA uses beds of activated carbon to polish drinking water before it is released for consumption. Because of its widespread use and the number of large manufacturers competing to make effective carbons, there is a sense within the environmental industry that all carbons are the same (Fan 2017). As detailed in previous sections, activated carbons are manufactured from a wide variety of raw materials, and they have very different properties. The example in Sect. 16.5 used design parameters associated with F400 high grade carbon derived from bituminous coal manufactured by Calgon Carbon. One of the more important characteristics

of AC is its adsorption capacity. This is a measure of the maximum mass of contaminant the carbon is capable of adsorbing at any given equilibrium concentration. The adsorption capacity is strongly dependent on contaminant concentration, the type of carbon (its source and activation method), and finally on the specific contaminant. There are organic compounds that are not adsorbed by AC at all. When dealing with multi-component products present at PHC sites, the adsorption dynamic becomes very complex, particularly in view of competitive desorption. Rules of thumb like AC can absorb roughly 15–20% by weight of organic contaminants are very misleading and should be discarded. PHC specific and AC product specific data should be relied upon.

One of the great advantages of AC is the ability to regenerate or reactivate spent carbons. Housekeeping on food-grade carbons is very good because when reactivated, the original customer will repurchase it. The same cannot be said for spent non-food-grade carbons. These carbons may originate from a multitude of sources ranging from wastewater to metal plating to manufacturing facilities. The reactivation process removes any organic contamination that may have been present, but inorganic contaminants will persist. Reactivated carbons that are not derived from food or drinking water applications should not be used for in-situ remediation because they may contain metal contaminants that could impact groundwater quality.

16.7 Microbial Growth on Carbon

16.7.1 Carbon Structure Providing Living Space

Natural organic matter, nutrient concentrations, and species richness decrease with depth, with notable increases in the transition zones such as the capillary fringe (Smith 2018). The typical decline in microbial abundance that accompanies increasing subsurface depth, at least in part, arises from decreasing transport pathways, the accompanying reduction in the influx of fresh organic carbon, and other required chemicals, such as electron donors or acceptors (Santamarina 2006). The size and shape of the cavities within the media and interstitial space between media grains restrain subsurface organisms' size, form, and mobility (Luckner 1991), and thus the population density. Population density is linked to the cavities and interstitial spaces, which are essential to the supply of nutrients, electron donors and acceptors, carbon sources, and the elimination of microbial metabolic wastes (Fredrickson 2001).

Essential requirements for subsurface microbial life include moisture, chemical factors such as electron donors, and media factors such as granularity. Since some of these elements are linked to the transport of water in the subsurface, microbial populations often reflect groundwater flow pathways (Maamar 2015; Graham 2017; Danczak 2018). The installation of AC into the subsurface by high-pressure, high-flow injection may establish new habitat by creating and expanding flow paths beyond that which existed in the native subsurface material (Lhotský 2021; CLU-IN U 2022).

The AC may accentuate water movement (Siegrist 1998; Sorenson 2019; ITRC 2020) due to the addition of three-dimensional networks of carbon seams and surfaces (Murdoch 1995; Bradner 2005; Or 2007). These seams can increase connectivity in the subsurface media as AC acts as a proppant holding the fractures open. The propped fractures can accommodate the introduction of additional microbes and microbial resources such as water and electron acceptors (Mangrich 2015; Zamulina 2020). Relatedly, AC's granular nature can also increase transport in the subsurface due to the formation of thick liquid films on the rough surfaces of AC (Or 2007; Massol-Deyá 1995). Together the AC seams and surfaces should support contaminant dispersion, movement of nutrients and terminal electron acceptors, the interchange of microbial metabolic products (Bures 2004), and microbial dispersal and colonization on newly accessible soil and aquifer compartments (Krüger 2019).

The surface of AC may provide recesses offering shelter for microbes, while its adsorptive properties enrich the environment of the AC with substrate (Weber et al. 1978). Microbial cells that inhabit the macropores and surface recesses are better sheltered against stressful environmental conditions, such as predation, than microbes in the native media (Kindzierski 1992; Żur 2016). Due to the surface recesses, more habitat exists for microbial growth (Liang et al. 2009). Concerning adsorptive capacity, by comparison to AC, organic resources in the subsurface are scattered within structurally heterogeneous media. AC consolidated resources result in higher substrate biodegradation and higher specific growth rates than non-adsorbing or weakly adsorbing media such as sand (Li 1983). Thus, AC consolidates organic resources (Weber et al. 1978) on a homogenous media, and microbes are drawn to the enriched environment of the AC (Liang 2007), which facilitates contact between degraders and contaminants (Chen 2012; Thies 2012; Bonaglia 2020).

It has long been observed that bacteria attach to and multiply upon the surface and in the macropores of AC (Board 1989; Morsen 1987; Liang 2008), and that biodegradation occurs on AC in the subsurface. (Peacock 2004) compared in-well coupons consisting of either glass wool or Bio-Sep® beads (75% PAC and 25% Nomex®) to investigate the in-situ bioreduction of technetium and uranium in a nitrate-contaminated aquifer. It was found that the beads supported microbes that reduced technetium and uranium, and the beads supported tenfold more microbial biomass than glass wool. It was stated that higher microbial biomass was most likely to exist due to the higher surface area of the beads and the concentration of nutrients on the beads as compared to the glass wool. Other studies have concluded that benzene, toluene, and phenol are effectively extracted from Bio-Sep® beads (Williams et al. 2013), metabolized by the microbes, and incorporated into fatty acids produced by microbes (Geyer 2005). Similar results were obtained for in-situ biodegradation of naphthalene at the McCormick and Baxter Superfund Site in Stockton, California (McCormick 2010). Nineteen well locations were tested, and all were positive for ^{13}C enrichment in the microbial lipid biomass.

PAC amended sediments in a microcosm study also demonstrated that bacteria attach to AC and multiply on the surface and within the macropores (Pagnozzi

2020). AC stimulated naphthalene biodegradation and mineralization under anaerobic conditions, as shown by the production of $^{14}CO_2$ from radiolabeled naphthalene (Pagnozzi 2021). The relative abundance of Geobacter, Thiobacillus, Sulfuricurvum, and methanogenic archaea, known to be associated with naphthalene degradation, increased after amendment with PAC. Under aerobic conditions, sediments containing 16 PAHs amended with PAC increased microbial community diversity, structure, and activity relative to both sand and clay controls. The alteration in the microbial community in response to PAC is consistent with that reported by Bonaglia (2020), who also examined and reported an increase in the biodegradation of high molecular weight PAHs for microbes associated with AC as did Acosta (Zapata Acosta 2019).

Furthermore, AC sustains microbial activity by decreasing toxic concentrations in the dissolved phase (Leglize 2008) and buffering the microbes against toxic shock (Sublette 1982). Specifically, the adsorption of PHCs onto AC significantly reduces their toxicity to microbes (Morsen 1990). The toxicity of petroleum compounds is reduced, as indicated by a sharp increase in the abundance of both native and inoculated petroleum degraders (Semenyuk 2014). Furthermore, AC added to sediments decreased toxicity as measured by ecological parameters (Kupryianchyk 2013). Likewise, adequately designed and deployed CBI should reduce contaminant toxicity to microbes.

16.7.2 AC Priming

Contaminant degradation is a function of the density of microbial microaggregates (Gonod 2006; Becker 2006). As discussed, AC installed in the subsurface is new habitat for microbial exploitation. Therefore, it may be advantageous to give hydrocarbon-degrading and degradation supporting microbes an opportunity to adhere to the AC before subsurface installation. This process is referred to as priming. Priming allows the AC to function as both a microbial inoculum delivery system and a readymade microbial habitat (Piai 2020). Similar approaches have proven successful in a variety of applications (Das 2017) and can result in more robust microbes (Meynet 2012) and microbial degradation that is sustained (Marchal 2013; Bonaglia 2020).

Priming stimulates formation of biofilms (term typically used to identify clusters of bacteria or archaea in a matrix of extracellular polymeric substances—EPS). Microorganisms embedded within biofilm achieve high resistance to toxic pollutants (Köhler 2006) and are durable, so biodegradation is persistent (Aktaş 2007; Ran 2018; Edwards 2013). In the subsurface, microbial-inoculated AC can establish a biofilm that promotes growth and diversity, degrades hydrocarbons and other contaminants, regenerates the AC, and persists over time (Lhotský 2021; Cho 2012). Figure 16.6 shows a case of microbial growth on AC in laboratory samples.

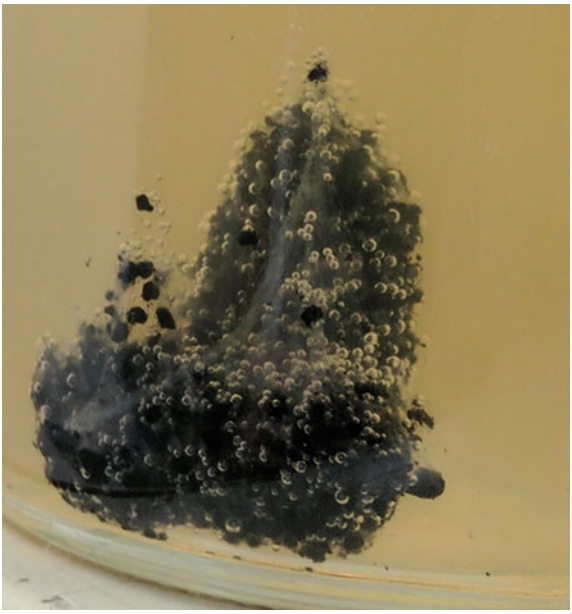

Fig. 16.6 Microbial growth on AC during a diesel bench test. A viscous material formed within days. The bubbles were gases produced by microbial activity

16.7.3 AC Adsorption as Barrier to Biodegradation

Studies have also shown that AC may have an inhibitory effect on microbial growth by decreasing the dissolved concentration of adsorbate available for microbial degradation. Marchal (2013) demonstrated for phenanthrene sorbed to soils that the stronger the adsorbent (AC, biochar, compost), the lower desorbed concentration, and the lower the microbial degradation (Marchal 2013). These results are not unique (Rhodes 2010), but they may be specific to adsorbates having high heats of adsorption like phenanthrene. Three-ring PAH, as is phenanthrene, degradation has been reported to be inhibited by AC, but 4 and 5-ring PAHs degradation is supported by AC (García-Delgado 2019). Aromatic compounds, having lower heats of adsorption, are not affected by AC to the degree reported for phenanthrene. Mangse (2020) found that AC carbon made toluene less bioavailable, but AC did not have a detrimental effect on toluene degradation (Mangse 2020). These observations are reasonable in that adsorbates that enter the AC are protected to some degree from biodegradation. The extent of that protection is influenced by the strength of the interaction with the AC. In the end, these observations follow from the adsorptive character of AC and they have not been demonstrated to be relevant to field application of AC, where multiple chemical adsorbates and NOM are present.

16.8 Evidence of Biodegradation at Sites with AC

16.8.1 Microbial Communities

Microbial attachment to AC is associated with an increase in the abundance of both native and inoculated petroleum degraders (Semenyuk 2014; Bonaglia 2020; Pagnozzi 2021). While the data to separate the function of AC from the CBI does not exist, an increase in microbial abundance is also associated with CBI emplacement. Figure 16.7 presents microbial data from groundwater samples collected from a CBI emplacement site 3 months post-emplacement. According to next-generation sequencing (NGS), the CBI emplaced sample has more total species, more individuals per species, and more rare species than either the control or the PHC impacted control. Figure 16.8 provides a stark visual confirmation of the abundance data presented in Fig. 16.7. More information on NGS can be found in Chap. 10.

A more definite question is whether the microbial populations in the CBI emplacement contain the individual microbes that are pertinent to PHC degradation. Figure 16.9 presents microbial data from groundwater collected from a CBI emplacement site 2 years post-emplacement. The microbial samples were examined

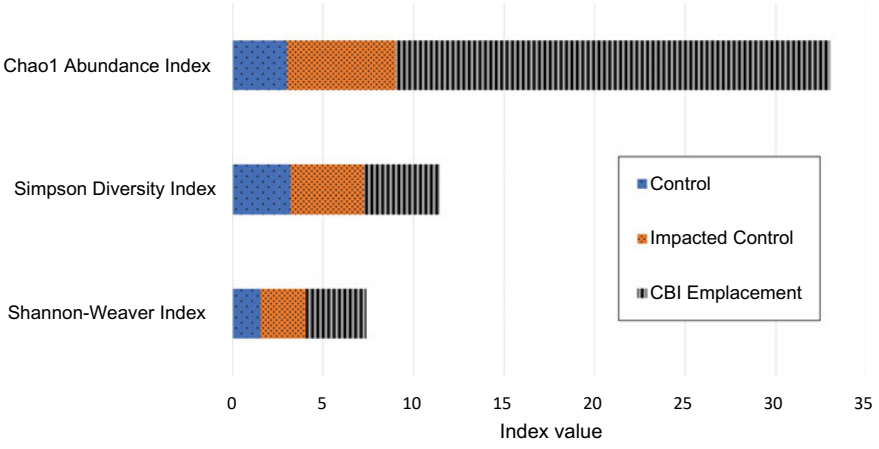

Fig. 16.7 Groundwater samples for both CBI treatment and controls analyzed by next-generation sequencing. Compared to controls, the CBI emplaced samples had more total species, more individuals per species, and more rare species. The Shannon–Weaver Index is the natural log of the total number of species in a sample. It reflects the total number of species present. The Simpson Diversity Index is the square of each species' abundance summed for the total sample population subtracted from 1; thus, proportional abundance is weighted more on the uniformity of individuals in the population, which is referred to as evenness. It indicates species dominance and reflects the probability of two individuals that belong to the same species being randomly selected. The scale is zero to 5, with 5 meaning that each species in a dataset is represented by the same number of individuals. The Chao1 abundance index is the number of individuals present and single or double individuals. It emphasizes individuals microbes present in small numbers

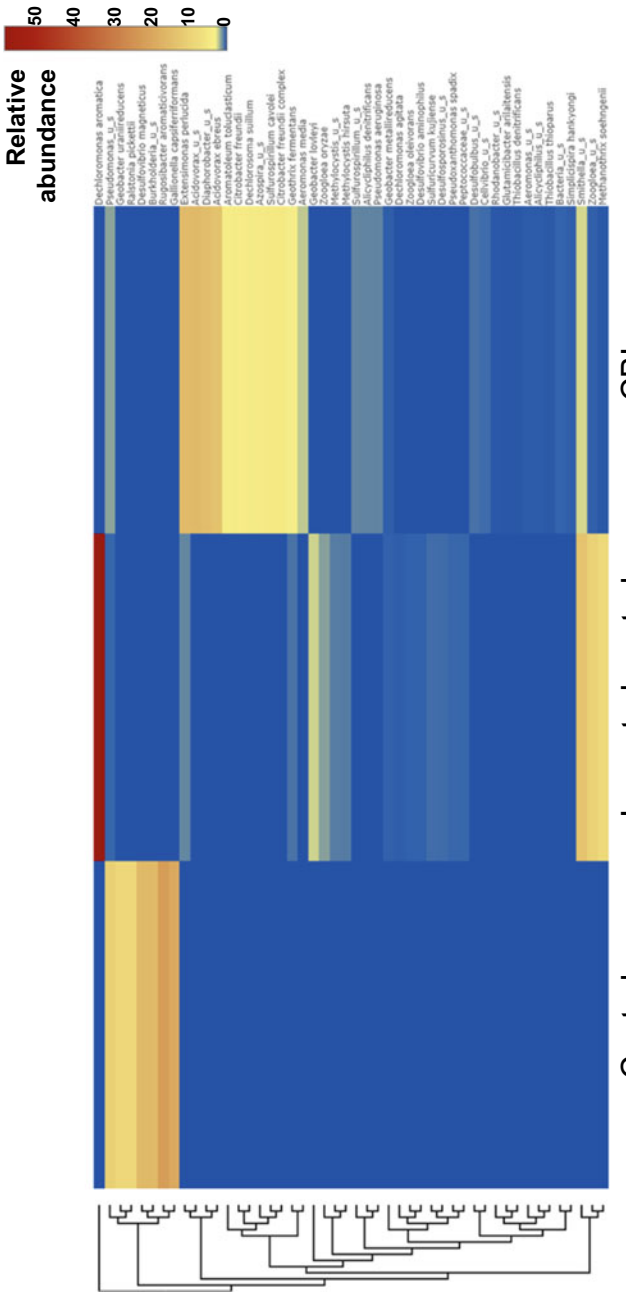

Fig. 16.8 Heat map presenting NGS microbial data at the species level by aligning taxa based on similarity. The three samples were from the same release site: the control sample was unimpacted by PHCs. The impacted control was impacted by PHCs but not treated with CBI. The CBI sample was drawn from an area in which CBI was emplaced. The colored scale indicated relative abundance taking into consideration genome size and number of reads

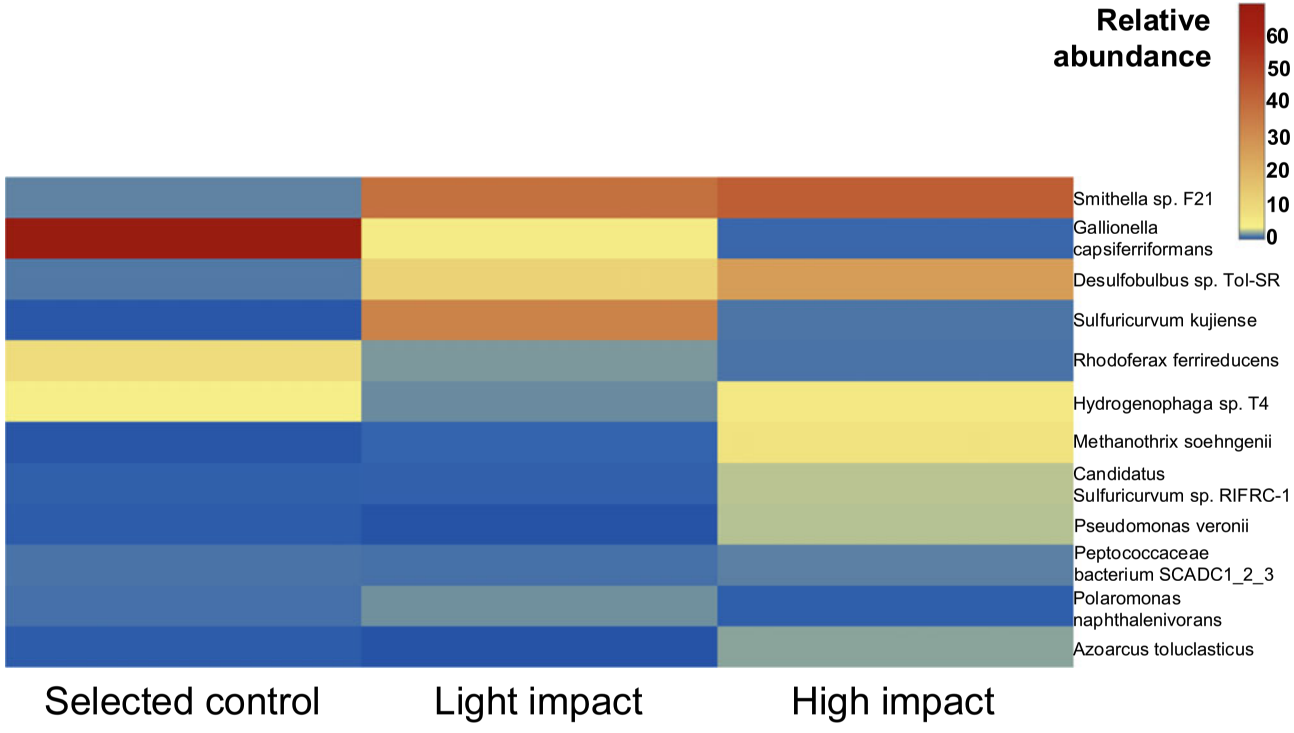

Fig. 16.9 NGS data displaying the most abundant twelve strains in samples within the CBI (BOS 200®) area. The colors in the columns and scale bar are relative intensity. The "control" sample was taken from the footprint of the injection but was intermittently impacted by petroleum. Due to site boundary constraints, an unimpacted control was not available. In the heavy impact sample, Smithella, Desulfobulbus, and Methanothrix are 48-, 36-, and 132-fold greater in absolute abundance than the low-impacted control

by NGS. Unambiguous control samples were not available. One side-gradient monitoring well, which had a history of intermittent PHC impacts, was selected as the best "control" available. Two consistently impacted monitoring wells were selected for comparison. All three monitoring wells were within the footprint of the in-situ injection of CBI. The samples were collected 2 years post-injection with a CBI containing nitrate and sulfate as electron acceptors. Added nitrates are short-lived being depleted in 1–3 months. The sulfate levels at the time of sampling ranged from 110 to 483 mg/L. The species that increased relative to the control monitoring well were catabolically and thermodynamically linked syntrophic communities. Figure 16.9 presents the most abundant species relative to the selected control. The colored scale indicated relative abundance taking into consideration genome size and number of reads. The most abundant microbes, Smithella, is a known alkane-degrading microbe (Ji 2020; Embree 2015). Under sulfate- and nitrate-reducing conditions, the primary condition at the site, Smithella degrades alkanes to acetate with the production of H_2 (Gieg 2014). *Desulfobulbus* sp. Tol-SR is distinguished by suites of genes (BSS, BBS, and BAM) associated with anaerobic toluene metabolism, which leads to acetate production (Laban 2015). Methanothrix utilizes acetate as a substrate for methanogenesis, while *Candidatus sulfuricurvum* derives energy from H_2 oxidation (Handley 2014). The connection between Smithella, Desulfobulbus, and H_2-utilizing methanogens is a typical hydrocarbon-degrading syntrophic relationship.

The difficulty with data presented in Fig. 16.9 is the lack of a control not impacted by PHCs. That does not prevent the observation that the microbes present were consistent with a petroleum degradation syntrophy. It does, however, make it difficult to determine how the CBI injection changed the population apart from the observation that the groundwater sample collected from the intermittently impacted monitoring well was less abundant than the samples drawn from the consistently impacted monitoring wells and that the microbial population present was capable of degrading PHCs.

The site data presented in Fig. 16.10 had appropriate control samples. The control samples were from areas that were not treated with CBI. Control 1 was drawn from an area that was unimpacted by PHC. Control 2 was drawn from an area impacted by PHC. Control 3 was drawn from an impacted area that bordered the CBI emplacement. It should be viewed as potentially influenced by the CBI. The three CBI emplacement groundwater samples were drawn from monitoring wells within the CBI treatment area. The samples were analyzed by NGS.

The microbial populations presented in Figs. 16.9 and 16.10 shared some characteristics. Smithella was the most consistently abundant microbe, but it was identified in all the impacted samples without regard to CBI emplacement status. Desulfobulbus was consistently present across the CBI emplaced samples. Methanothrix soehngenii was present but not confined to the CBI emplacement samples. *Candidatus sulfuricurvum* was not present. Two microbes absent from the Fig. 16.9 site were present at the Fig. 16.10 site. *Geobacter metallireducens* was present in the CBI samples and control 3, which was about 3 m from the CBI emplacement. *Geothrix fermentans* was present in the same pattern. *Geobacter metallireducens* uses electron donors such as acetate and uses Fe(III) as an electron acceptor (Coates 1999). *Geobacter*

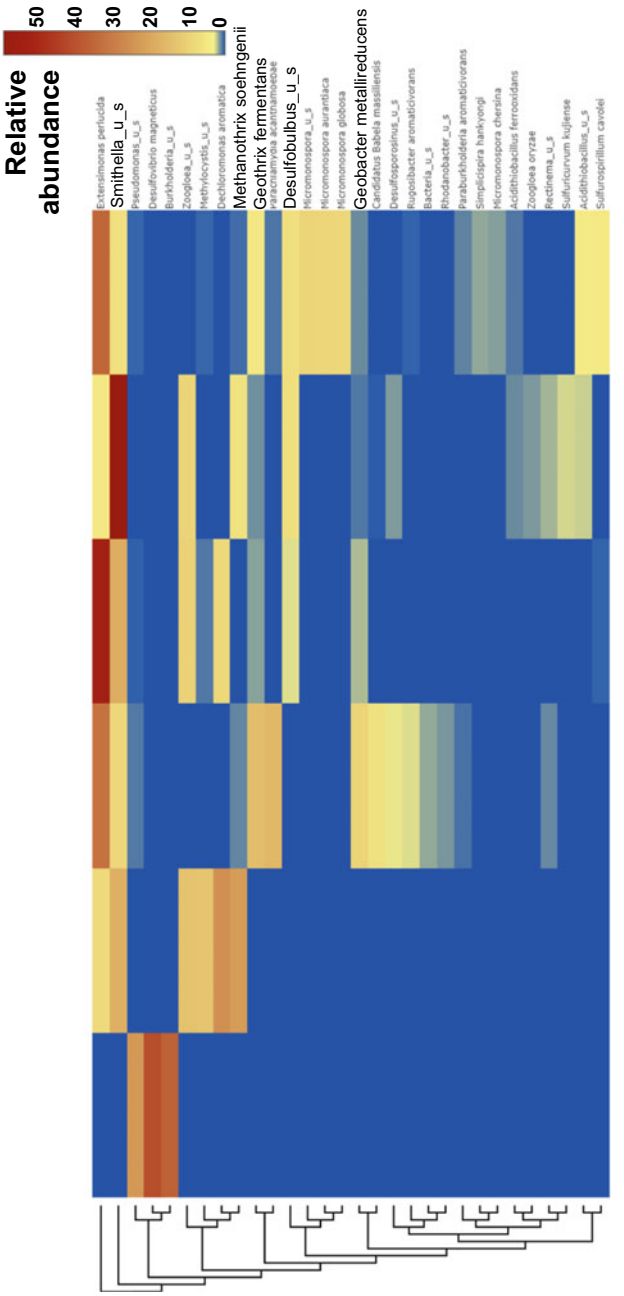

Fig. 16.10 NGS data from monitoring wells. The data is displayed at the species level. Multiple controls are present. Control 1 was drawn from an area that was unimpacted by PHC. Control 2 was drawn from an impacted area. Control 3 was drawn from an impacted area that bordered the CBI emplacement and should be viewed as potentially influenced by the CBI. The three CBI samples (CBI 1–3) were drawn from monitoring wells within the CBI emplacement. Smithella and Desulfobulbus were elevated relative to control. Methanothrix, however, did not have a consistent pattern. In this dataset, Geothrix and Geobacter were elevated

metallireducens couples the oxidation of aromatic compounds to the reduction of Fe(III)-oxides (Butler 2007), but acetate and ethanol are preferred over benzoate, although, benzoate is co-consumed with toluene and butyrate (Marozava 2014). These microbes are known to participate in direct interspecies electron transfer (DIET) using the AC. And the presence of these microbes may establish a second syntropic pathway to oxidize acetate and reduce CO_2 (Rotaru 2018). Both sites had a microbial population capable of degrading PHCs.

While describing the microbes present in the monitoring wells 2–3 years' post-injection and demonstrating that they were consistent with a hydrocarbon-degrading syntrophy is a good qualitative indicator of biodegradation in response to a CBI, the presence of genes encoding hydrocarbon enzymes in a microbial population can also be used to characterize biodegradation potential. Figure 16.11 presents qPCR data (QuantArray®-Petro from Microbial Insights, Inc.). The array quantifies a select suite of 25 functional genes involved in aerobic and anaerobic biodegradation of PHCs. Samples were collected from unimpacted monitoring wells and from impacted monitoring wells prior to injection with CBI (BOS 200®). Of the 25 functional genes, five of them were not present in any of the samples. Of the remaining 21, eight function genes were present in the unimpacted background, six additional ones were expressed in the impacted background post-injection, and post-inject seven additional function genes were observed. No identified function genes were lost by the first-month post-injection. Two previously identified functional genes were not identified at month five. At month five, 19 of the 21 quantified function genes were observed and on average the microbial count using the functional genes as markers increased 56-fold in cells/ml (range from 3.4 to 178.5-fold cells/ml). The average and range did not include three functional genes that increased from a low estimated value to 106-fold the estimated value. The gene array demonstrated that, for the period examined, the petroleum-degrading population expanded post-injection of CBI relative to both impacted and unimpacted controls. More information on qPCR can be found in Chap. 10.

Examining a subset of the data from Fig. 16.11, benzylsuccinate synthase (BSS in the QuantArray®) catalyzes the addition of fumarate to toluene (Biegert 1996) and potentially the monoaromatics xylene and ethylbenzene (Kharey 2020) to generate benzylsuccinate, the first step in anaerobic toluene metabolism (Biegert 1996). Benzylsuccinate becomes benzoyl-CoA and succinyl-CoA. Succinyl-CoA is recycled back to fumarate, while benzoyl-CoA proceeds through benzoyl-CoA reductase (BCR in the QuantArray®) to acetate, a small fatty acid easily used by many microbes. This is the toluene anaerobic pathway previously described above for site presented in Fig. 16.9. Thus, a selected subset of the gene expression from the Fig. 16.11 site provides a similar picture in Fig. 16.9 and has overlap to the site presented in Fig. 16.10. Other enzymes coding genes, associated with both aerobic and anaerobic pathways, are increased in number post-CBI emplacement, and the total microbial count in the impacted area also increases post-injection (Fig. 16.11) Notice that the total eubacteria, sulfate-reducing bacteria, iron-reducing bacteria, and denitrifying bacteria are increased more than tenfold. Thus, the release site presented in Fig. 16.11 confirms that CBI emplacement increases microbial abundance, increases microbes

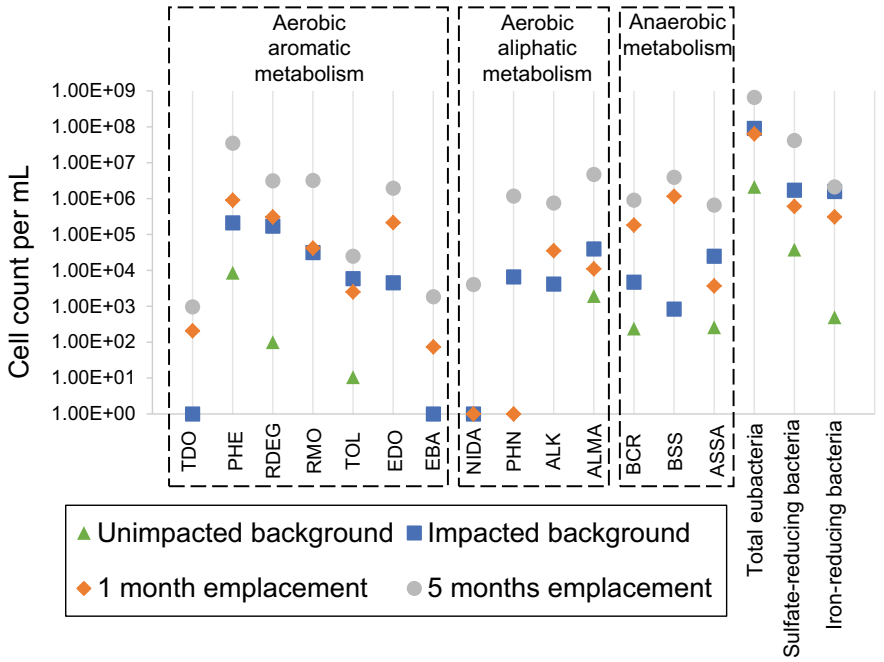

Fig. 16.11 QuantArray®-Petro data from a site where CBI was injected. Microbes having selected genes associated with both aerobic and anaerobic petroleum hydrocarbon metabolism increased in number relative to background. The increase was higher at 5 months post-emplacement than at 1 month

having genes known to be important in PHC degradation, and confirms the data conclusions drawn from Figs. 16.8, 16.9, and 16.10.

16.8.2 Additional Lines of Evidence of Microbial Activity

16.8.2.1 Decrease in Electron Acceptors and Increase in Gases

For CBI that provide electron acceptors, decreasing concentration in potential electron acceptors (such as oxygen, nitrate, and sulfate) is indicative of microbial activity. Figure 16.12 is from a petroleum release site. The decrease in electron acceptors followed an often-observed pattern. Contaminant concentration significantly decreased upon installation of CBI. Early post-emplacement, the system reaches equilibrium. When electron acceptors such as sulfate and nitrate were added with

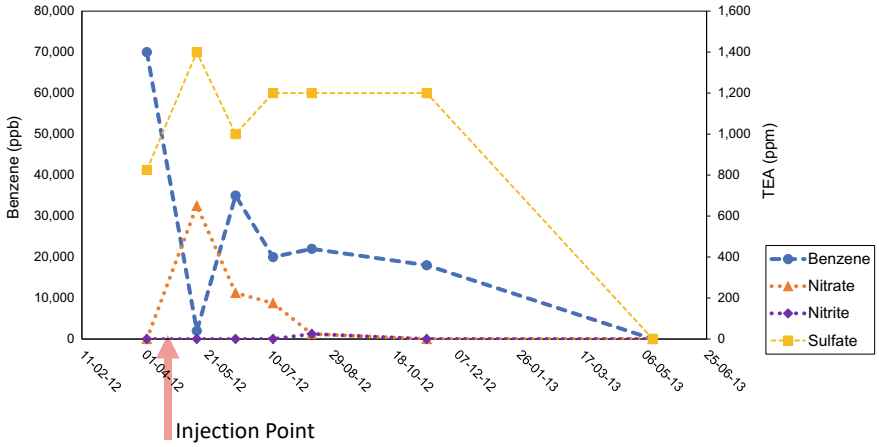

Fig. 16.12 Electron acceptors at a site where CBI was installed. Nitrate concentrations dropped first followed by a slight rise in nitrite. Sulfate concentrations persisted longer. Benzene concentrations were added to the graph for comparison

the AC, nitrate concentrations decreased quickly, leading to a slight, transient elevation of nitrite. Sulfate dropped slowly over time. The nitrate and sulfate consumption patterns were consistent with anaerobic metabolism using nitrate and sulfate as electron acceptors.

Increasing respiration products (such as CO_2, Fe(II), sulfide, and CH_4) is also consistent with microbial activity. Figure 16.13 demonstrates the rising concentration of methane (associated to anaerobic biodegradation processes as explained in Chap. 5) and other gases at a site where CBI was installed.

16.8.2.2 Decreasing Concentrations in Soil and Groundwater

The most often presented data to demonstrate decreases in contaminant concentrations are monitoring well data. Figure 16.5 depicted a typical groundwater concentration pattern after subsurface CBI emplacement. Figure 16.14 presents groundwater data for benzene and TVPH post in-situ emplacement of CBI. Contaminant concentrations in groundwater decrease due to PHCs adsorption onto the AC. The most water-soluble constituents can move into the AC quickly, but those same constituents may have lower heats of adsorption than constituents presenting a lower solubility, so there is a period over which a new equilibrium is established. The total amount of contamination relative to the AC determines the time it will take to reach equilibrium. From that point forward biodegradation controls the final phase of site remediation.

Core samples collected periodically at adjacent locations from sites treated with CBI typically show a decrease in contaminant concentration in soil, often exhibiting consistent patterns despite the high variability commonly associated to physical sampling of soil and aquifer materials. Figure 16.15a present ethylbenzene data

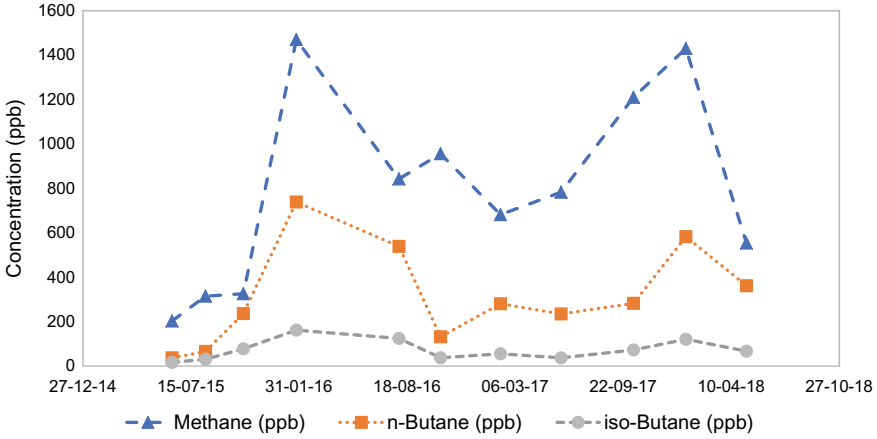

Fig. 16.13 Prior to injection, which was completed in June of 2015, gases, except for methane, were not detected above detection limits. Three months post-CBI emplacement, the concentration of gases linked to microbial metabolism like methane, *n*-Butane, and iso-Butane rose. Gases such as cis-2-Butene, propane, ethane, *t*-2-Butene, 1-Butene, and iso-Butylene (not displayed) exhibited similar patterns

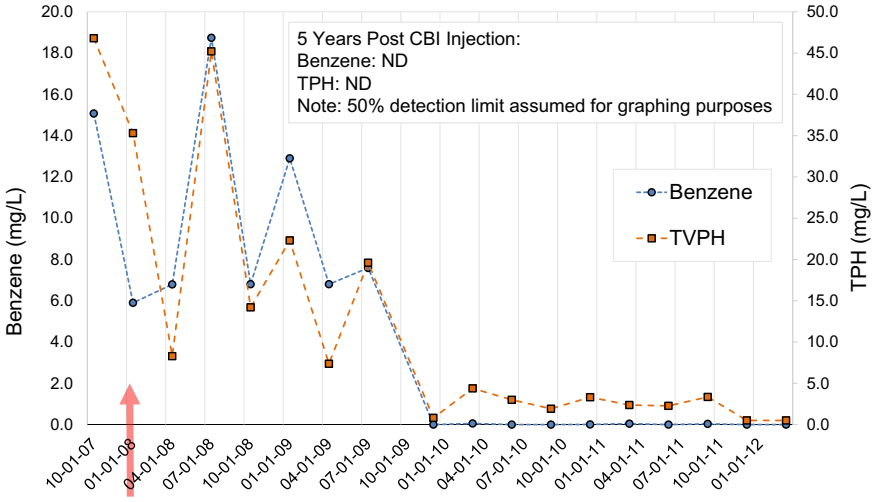

Fig. 16.14 The red arrow marks the injection of the CBI BOS 200®. The initial decrease in TVPH concentrations was followed by a re-equilibration phase. Biodegradation may have initiated early post-CBI emplacement but did not seem to dominate the PHC concentration pattern until the final stages of site remediation

a)

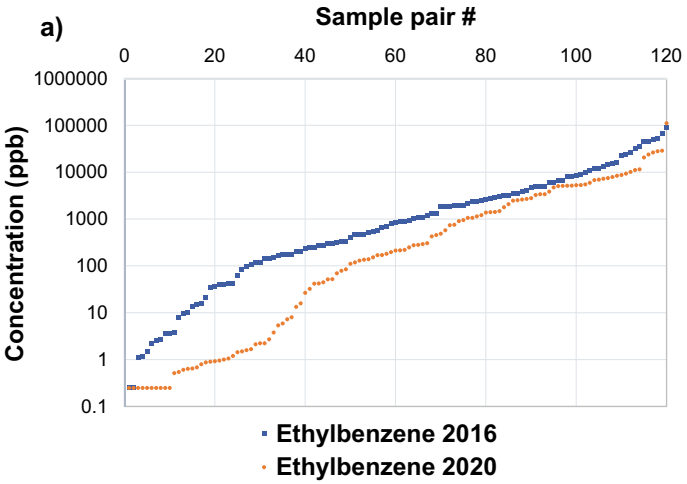

b)

Raw Statistics		
40 Months	**2016**	**2020**
Number of Valid Observations	120	120
Number of Distinct Observations	115	109
Minimum (Detection Limit)	0.25	0.25
Maximum	91100	112000
Mean	6285	3628
Median	866.5	215.5
Standard Deviation	14165	11431
Standard Error of Mean	1293	1044
Wilcoxon-Mann-Whitney (WMW) Test		
H0: Mean/Median of 2016 <= Mean/Median of 2020		
P-Value (Adjusted for Ties)	**9.38E-04**	
Conclusion with Alpha = 0.05		
Reject H0, Conclude 2016 > 2020		

c)

Constituent	Median Difference	P-value
Benzene	3.6 fold lower	0.0009
Toluene	1.5 fold lower	0.0018
Ethylbenzene	4.0 fold lower	0.0009
m/p Xylene	2.2 fold lower	0.0091
o-Xylene	2.5 fold lower	0.019
1,2,4-TMB	1.2 fold lower	0.0289
Naphthalene	3.5 fold lower	0.0019

Fig. 16.15 Ethylbenzene concentration from soil samples was significantly lower in 2020 than in 2016. All other PHCs analyzed were also significantly lower in the 2020 soil samples than in the 2016 soil samples

from a BOS 200® in-situ injection into fat clay geology at an LNAPL site. The raw statistics for ethylbenzene shown in Fig. 16.15b are illustrative of the data for all other contaminants examined from the same site. All constituents examined were significantly decreased in concentration in the aquifer solids tested at 40 months (see Fig. 16.15c).

16.8.2.3 Compound-Specific Isotope Analysis (CSIA)

As discussed in Chap. 11, CSIA tracks the stable isotope composition of selected volatile organic compounds (VOCs) to obtain information on attenuation processes. In tracking the degradation of benzene due to biological degradation, benzene should become increasingly enriched for 13C isotopes as the benzene containing 12C isotopes preferentially has its carbon bond broken.

The international standard for the ratio of 13C–12C isotopes is the Pee Dee Belemite (PDB) standard and is 0.01123720 (IAEA 1993). So about 1% is 13C and 99% is 12C. To determine if biodegradation is indicated, one can measure the increase in 13C above the PDB standard. It has become convention to present the change (δ) in 13C, (δ13C) as the isotopic ratio of the sample (Rs) divided by the isotopic ratio of the standard (Rstd) (Meckenstock 1999; Hayes 2004). Next, because the fraction is small the value is multiplied by 1000 to shift the decimal place and present the data as part per thousand often reported as permill (‰). Thus, for isotopic data presented as the δ13C, as δ13C moves closer to zero the value becomes less negative because the molecules are enriched for δ13C. See Eq. 16.4 from (Mackenstock 2004).

$$\delta 13C(‰) = (Rs/Rstd - 1) \times 1000$$

$$(Rs/Rstd) = [(13C/12C)s - (13C/12C)std]/(13C/12C)std \tag{16.5}$$

In Fig. 16.16, δ13C enrichment data are presented form a CBI injected site. To determine if benzene sorbed to the formation was being degraded, impacted but untreated core samples were collected in a benzene impacted area upgradient of the CBI emplacement and within the CBI emplacement area. These samples were examined for isotopic carbon enrichment under the assumption that the upgradient and downgradient samples were immediately connected by a shared flow path. The isotopic fractionation from the extracted mass indicated enrichment for δ13C in the downgradient, within the injection area, smear zone samples. The difference between three of the four points exceeds $\delta 13C \geq 2‰$. The data were indicative of biodegradation.

To compare δ13C enrichment prior to interaction with the CBI emplacement versus the isotopic enrichment post interaction with the CBI emplacement, a stable isotope enrichment factor, epsilon (ε), may be calculated (see Eq. 16.7). The calculated epsilon for the data presented in Fig. 16.16 is $(\varepsilon) = -3.5$. This value is consistent with the stable isotope enrichment factors reported for a sulfate-reducing culture,

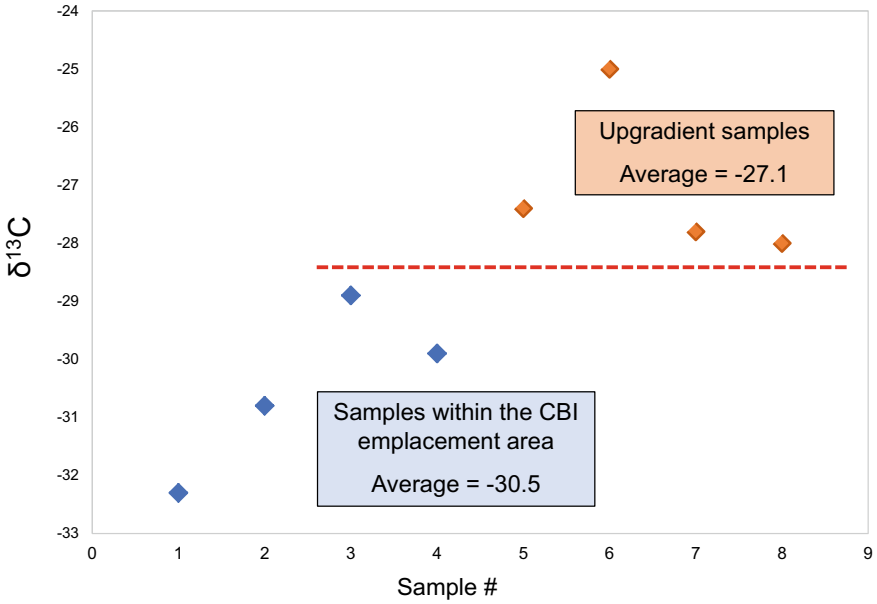

Fig. 16.16 Core samples were collected from a CBI emplacement on a petroleum release site. Points below the red line were upgradient of the CBI emplacement. Points above the red line were samples collected within the CBI emplacement. The data are indicative of biodegradation

which ranges from -2.7 to -3.6 (Mancini 2003). The CBI used, BOS 200®, contains significant sulfate; thus, the ε value is consistent with expectations and indicated biodegradation.

$$\varepsilon = \left\{ \left[\frac{(1000 + \delta 13\text{Cprior})}{1000 + \delta 13\text{Cpost}} \right] - 1 \right\} \times 1000 \tag{16.7}$$

To be thorough, neither abiotic nor non-degradative processes are known to result in significant stable isotopic fractionation of benzene relative to biological processes. Non-degradative processes such as sorption, volatilization, and dissolution are typically smaller than the analytical uncertainty associated with CSIA, which has been reported as ± 0.5‰ (Hunkeler 2008). Specifically, the sorption of benzene to activated carbon does not result in stable isotope fraction greater than this ± 0.5‰ accuracy (Slater 2000; Schüth 2003). Abiotic degradation processes associated with benzene can be similarly disregarded. Plotting the carbon stable isotope concentration δ13C against the natural logarithm of the concentration can be used to support that a single process is the main control behind the change in contaminant concentration (Hunkeler 2008).

Data from another site where CSIA was conducted are presented in Fig. 16.17, which depicts a sustained reduction of BTEX contamination downgradient of a CBI PRB despite BTEX continuing to enter the barrier from the upgradient side.

The CBI PBR was installed because an existing groundwater extraction and re-injection system was failing to perform. CSIA was conducted to determine whether the decrease in concentration was due only to adsorption to the AC or if the decrease was also affected by biodegradation. Groundwater samples were collected from monitoring wells located on a transect through the CBI PBR. The monitoring well upgradient of the CBI PBR was impacted by the same PHCs as the monitoring wells downgradient of the CBI PBR. The groundwater extraction and re-injection system remained active after the CBI PBR was installed. It withdrew groundwater from a series of wells located ~55 m downgradient from the control monitoring well and re-injects oxygenated water at ~18 m upgradient from the same control well.

Figure 16.18 shows δ13C enrichment data. Of the five VOCs examined by CSIA, three (*n*-propylbenzene, ethylbenzene, m,p-xylene) were enriched, greater than analytical uncertainty, relative to the upgradient monitoring well. O-xylene did not demonstrate enrichment, and 1,2,4-trimethylbenzene enrichment was within laboratory error (data not shown). Determining the cause of the observed isotopic enrichment was complicated by the presence of the extraction and re-injection wells because re-injection may enhance degradation by oxygenating the re-injected groundwater. Nevertheless, enrichment is indicated.

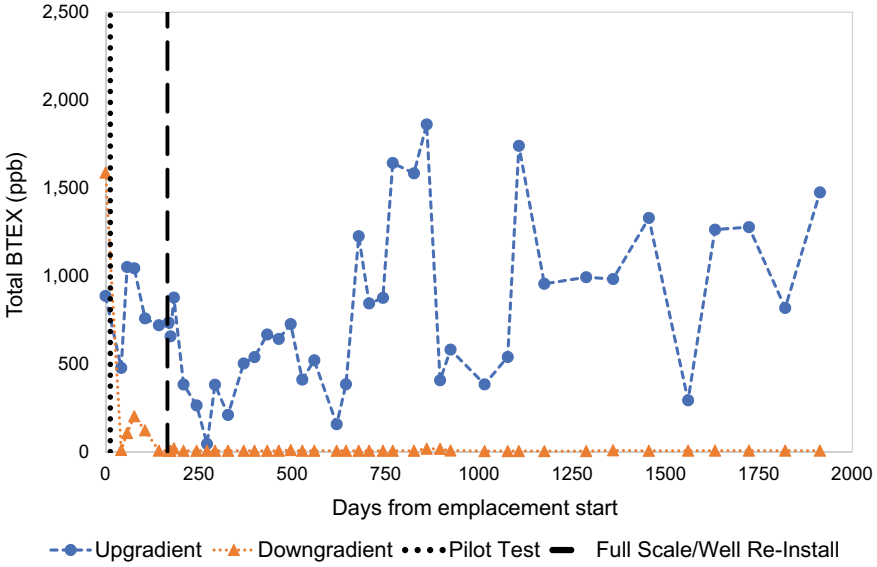

Fig. 16.17 Groundwater sampling data from upgradient and downgradient of emplaced PRB. BTEX on the downgradient side of the barrier remains suppressed despite BTEX continuing to enter the barrier from the upgradient side

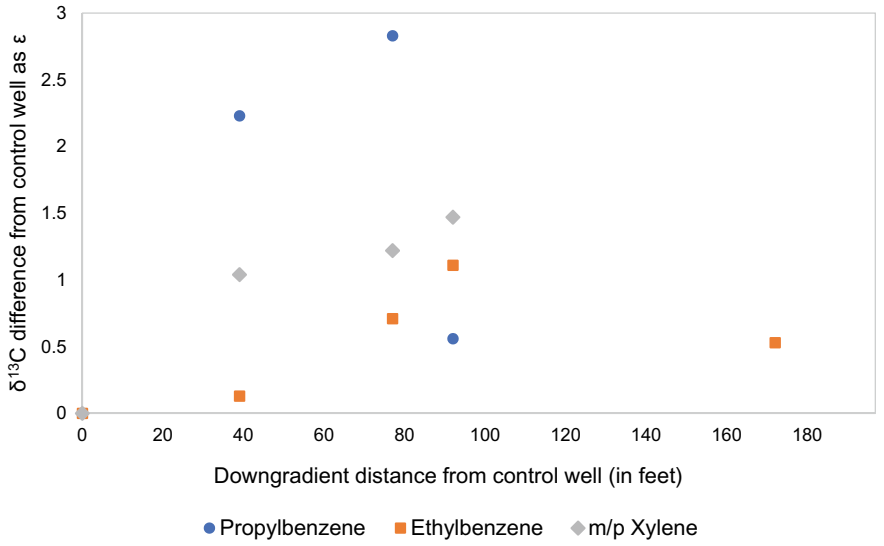

Fig. 16.18 Samples of groundwater collected upgradient of a PRB and at multiple distances downgradient. *N*-propylbenzene, ethylbenzene, and *m*, *p*-xylene showed 13C enrichment. The results indicated the occurrence of biodegradation by having an enrichment of δ13C ≥ 1‰

16.9 Biological Regeneration

As a general process, biological regeneration (BR) of AC is well documented (Aktaş 2007; El Gamal 2018). Adsorption, biofilm formation, and biodegradation can occur simultaneously on AC (Piai 2020; Betsholtz 2021), with the combination of microorganisms and the adsorptive capacity of AC being synergistic in promoting BR (Nath 2011a, b). Upon emplacement in the subsurface, AC in CBIs adsorbs hydrophobic chemicals such as PHCs and natural organics. Microbes in the resource-rich regions near the AC bloom. As the biomass on the AC expands, desorption (Leglize 2008; Ying 2015) and regeneration rates increase (Betsholtz 2021) such that the adsorptive capacity of AC is extended (Chan 2018; Piai 2022). In time, some of the products of degradation as well as natural organics fill a percentage of the AC micropores, but they have not been demonstrated to either completely fill the micropores nor cause biodegradation to cease (Smolin 2020; Díaz de León 2021). This general scenario has been developed from in vitro experiments and the examination AC used in water treatment (FRTR 2021; El Gamal 2018). The development of microbial growth on AC is referred to as biologically activated carbon (BAC). The development of BAC is well documented and has been presumed to specifically occur on AC in CBIs emplaced in the subsurface (Regenesis 2022).

The specific source material (coal, coconut, etc.), activation method (Coelho 2006), and particle size (GAC, PAC, colloidal) (El Gamal 2018) all influence BR. For example, coconut carbon does not bioregenerate as well as wood-based (Piai 2019)

or coal-based AC (Zhang 2013). The activation method, e.g., chemical versus physical, influences the AC's surface area, pore type distribution, and adsorptive capacity, which all affect BR. As concerning particle size, BR has been demonstrated for GAC and PAC (El Gamal 2018). Generally, increasing particle size lowers substrate diffusion within the biofilm while increasing biodegradation (Liang 2007; Rattier 2012; El Gamal 2018).

AC porosity is likely the most important characteristic influencing both the rate and extent of AC BR (El Gamal 2018; Lu 2020; Aktaş 2007). Larger pores generally support BR (Aktaş 2007; Díaz de León 2021) and may provide microbes, enzymes, and surfactants with more access to the micropores or better habitat for microbes. The microbial community that develops on AC is influenced by the pore structure and the compounds available for biological degradation (Yu 2021).

Individual chemicals vary in how they affect the degree and rate of BR (Nath 2011a, b; Chan 2018). The biodegradability of a specific contaminant varies due to molecular structure among other factors (Cirja 2008). In general, large molecular weight compounds having low heats of adsorption are biodegraded easier than small molecules having high heats of adsorption (García-Delgado 2019).

The influence of multiple factors makes it difficult to estimate the degree to which AC can be recycled. The percent of dissolved organic carbon (DOC) degraded by biological activity varies from 25 to 42% (Fundneider 2021). Bioregeneration ranges from 12 to 95% (Nath 2011a, b). The percentages of pore restoration reported in the literature are broad (Aktaş 2007; Nath 2011a, b). A model system of biofilm on AC degrading 2-nitrophenol was run for 38 months after which it was reported that 39% of the initial pore volume was still available (Smolin 2020). Thus, AC is not typically fully restored by microbial regeneration. This may be due to binding products of microbial metabolism and non-organic carbon (Smolin 2020; Díaz de León 2021). Nevertheless, the apparent adsorption capacity of microbial biofilm on AC exceeds that of the AC alone.

16.9.1 Process of Bioregeneration: Adsorption–Desorption, Exoenzymes, and Surfactants

It has been argued that biodegradation occurs in the dissolved phase external to the AC after which the PHCs or other chemicals on the AC re-equilibrate with the dissolved phase (de Jonge 1996; Abromaitis 2016; Díaz de León 2021). However, not all chemicals that bind to AC are released with equal ease (Nath 2011a, b) or released as rapidly as BR has been reported to occur (Piai 2021). Therefore, this process is insufficient to explain BR of AC.

Conceivably, multiple processes are involved in BR, including adsorption and desorption and the participation of exoenzymes (Perrotti 1974) and surfactants (Marchal 2013; Edwards 2013). Biofilm producing microbes have been demonstrated to degrade phenanthrene adsorbed to AC, while non-biofilm forming microbes failed

to do so (Leglize 2008). Microbes create a scaffolding made of EPS, which adheres to surfaces and allows microbes to build a biofilm habitat that supports microbial cooperation. One aspect of the formation of the biofilm habitat is the ability for the microbes to release extracellular enzymes (exoenzymes) into the biofilm forming a kind of extracellular digestive system (Flemming 2010).

The exoenzyme hypothesis proposes that enzymes secreted by the bacteria diffuse into the micropores and catalyze a transformation that desorbs the adsorbate from the micropores so that it moves out of the AC (Perrotti 1974; Nath 2011a, b). The argument against the exoenzyme theory is that enzymes are too large to enter the micropores (Xiaojian 1991), which is generally correct since most enzymes range from 3 to 7 nm in diameter if viewed as a sphere (Erickson 2009). However, it may not be necessary for the exoenzymes to enter the micropores. Focusing on the aqueous phase versus the adsorbed phase may overlook biocenoses within the biofilm. If the concentration of PHCs is reduced in spaces within the biofilm, PHCs may be released from the micropores (Klimenko 2003a, b) and be degraded within the extracellular space. The release of PHCs from AC may be enhanced by the presence of biosurfactants, which are also common in biofilms and have been demonstrated to facilitate BR (Klimenko 2003a, b).

16.9.2 Diet

It has been proposed that PHCs in the micropores of AC are still available for biodegradation through DIET (Liu 2012; Summers 2010). Under methanogenic conditions, the biodegradation of PHCs requires the syntrophic cooperation between bacteria and archaea (Gieg 2014). Syntropic bacteria oxidize PHCs to CO_2, H_2, and acetate (Kim 2019). The methanogenic archaea remove the hydrogen, which helps the fermenters because the fermentation reaction is only thermodynamically favorable at low hydrogen ion concentrations (Barton 2005; Dolfing 2008). Microbial interactions whereby electrons are exchanged through intermediates such as hydrogen and acetate are well described (Kim 2019). A substantial body of evidence, however, supports that electron exchange can occur without chemical intermediates, also in the case of bacteria and methane-producing archaea (Summers 2010; Chen 2022), also in the case of bacteria and methane-producing archaea (Lovley 2017; Yee 2019). As a result of this process, bacteria may not need to be in direct contact with PHCs to be able to degrade them.

16.9.3 Conclusions and Future Research Needs

While the general efficacy of AC and the derived CBIs has been demonstrated in field applications and laboratory studies, further research is needed. Failure to meet remediation goals occasionally occurs. Most of those failures are due to insufficient

site characterization and inadequate distribution of the CBI within the hydrocarbon mass. Therefore, technological improvements are needed to optimize remedial design characterization and CBI installation. Further research is also encouraged to better understand the adsorption–desorption mechanisms of different AC types for in-situ remediation of PHC fuel mixtures.

On the biological side, how the syntrophic relationships form, which individuals become most numerous in the syntrophy, and how the relationships evolve as degradation proceeds are appreciated, but more needs to be done to understand these processes in CBI treatment zones as well as questions like whether co-injection of bacterial consortia significantly improves performance and how indigenous microbes interact under bioaugmentation. Further metagenomic and CSIA studies across hydrocarbon types and geological settings could be enlightening. The cooccurrence of microorganisms has helped unwind some associations, but employing transcriptomics and proteomics will move us beyond descriptions or cooccurrences.

High contaminant concentrations and NAPLs are difficult to bioremediate quickly. The capacity of AC to adsorb contaminants thereby lowering dissolved phase contamination can decrease the negative impacts to the soil biota by hydrocarbon contamination. Adsorption onto AC can reduce the bioavailability and, thus, the toxicity of hydrocarbons to subsurface microbes (Meynet 2012). While the adsorptive capacity is helpful and biodegradation proceeds despite the presence of NAPL, the remediation market craves faster degradation rates. Therefore, optimization of both products and installation practices to increase the rate of NAPL degradation is a pertinent area of research.

On the other hand, many remediation technologies that are initially successful with fuel hydrocarbons suffer from mediocre performance when contaminant concentration becomes low. For example, MTBE is very soluble in water. Consequently, it moves readily with groundwater and often creates expansive low concentration plumes. Biodegradation will stall as the concentration of the MTBE drops too low to sustain a robust population of microbial degraders (USEPA 1999; Muller 2007; Li 2014). AC overcomes this limitation by concentrating the oxygenate in its pores. Optimizing CBI remedies to address very low-concentration plumes is an additional area of research.

AC is versatile and will function under aerobic or anaerobic conditions. Mixers used to prepare CBI slurries typically entrain air and oxygenate the water. AC readily adsorbs dissolved oxygen, so the state within the pore structure is aerobic at the time of injection. This feature suggests that injection of CBI at sites where sparging systems are installed may significantly enhance remedial performance. Typical sparging systems are inefficient as most of the oxygen added is lost in the vapor leaving the saturated formation. The addition of AC may enhance sparging efficiency because of its ability to adsorb oxygen. This illustrates the possibility of many different applications of AC in subsurface remediation that are yet to be considered or investigated.

References

Abromaitis VR (2016) Biodegradation of persistent organics can overcome adsorption–desorption hysteresis in biological activated carbon systems. Chemosphere 149:183–189. https://doi.org/10.1016/j.chemosphere.2016.01.085

Aktaş OA (2007) Adsorption, desorption and bioregeneration in the treatment of 2-chlorophenol with activated carbon. J Hazard Mater 59(4):769–777. https://doi.org/10.1016/j.ibiod.2007.01.003

Barton L (2005) Structural and functional relationships in prokaryotes. Springer, New York

Becker JM (2006) Bacterial activity, community structure, and centimeter-scale spatial heterogeneity in contaminated soil. Microb Ecol 51:220–231. https://doi.org/10.1007/s00248-005-0002-9

Betsholtz AK (2021) Tracking 14C-labeled organic micropollutants to differentiate between adsorption and degradation in GAC and biofilm processes. Environ Sci Technol 55(15):11318–11327. https://doi.org/10.1021/acs.est.1c02728

Biegert TFG (1996) Evidence that anaerobic oxidation of toluene in the denitrifying bacterium *Thauera aromatica* is initiated by formation of benzylsuccinate from toluene and fumarate. J Biochem 238(3):661–668. https://doi.org/10.1111/j.1432-1033.1996.0661w.x

Board TW (1989) Final report hazardous waste management approaches to protect water quality. Texas Water Developmnet Board, Austin. https://www.twdb.texas.gov/publications/reports/contracted_reports/doc/8483541.pdf

Bonaglia SB (2020) Activated carbon stimulates microbial diversity and PAH biodegradation under anaerobic conditions in oil-polluted sediments. Chemoshpere 248:126023. https://doi.org/10.1016/j.chemosphere.2020.126023

Bradner GM (2005) Effects of skin and hydraulic fractures on the performance of an SVE well. J Contam Hydrol 77:271–297. https://doi.org/10.1016/j.jconhyd.2005.02.001

Bures G (2004) Assessment of chitin distribution and fracture propagation during bio-fracingTM. Remediation of chlorinated and recalcitrant compounds—2004. In: Proceedings of the fourth international conference on remediation of chlorinated and recalcitrant compounds. Battelle, Monterey, CA. https://projects.battelle.org/chlorinated-conference/2004Chlor_Proceedings/Papers/3D-22.pdf

Butler JH (2007) Genomic and microarray analysis of aromatics degradation in *G. metallireducens* and comparison to a Geobacter isolate from a contaminated field site. BMC Genom 8:180. https://doi.org/10.1186/1471-2164-8-180

Chan PL (2018) Bioregeneration of granular activated carbon loaded with phenolic compounds: effects of biological and physico-chemical factors. Int J Environ Sci 15(8):1699–1712. https://doi.org/10.1007/s13762-017-1527-4

Chen BY (2012) Enhanced bioremediation of PAH-contaminated soil by immobilized bacteria with plant residue and biochar as carriers. J Soils Sedim 14:1350–1359. https://doi.org/10.1007/s11368-012-0554-5

Chen LF (2022) Improvement of direct interspecies electron transfer via adding conductive materials in anaerobic digestion: mechanisms, performances, and challenges. Front Microbiol 13:1051. https://doi.org/10.3389/fmicb.2022.860749

Cheremisinoff PN (1978) Carbon adsorption handbook. Ann Arbor Science Publishers, Ann Arbor

Cho Y-MW-J (2012) Long-term monitoring and modeling of the mass transfer of polychlorinated biphenyls in sediment following pilot-scale in-situ amendment with activated carbon. J Contam Hydrol 129:25–37. https://doi.org/10.1016/j.jconhyd.2011.09.009

Christiansen CM (2010) Comparison of delivery methods for enhanced in situ remediation in clay till. Groundwater Monit Remed 30(4):107–122. https://doi.org/10.1111/j1745-6592.2010.01314.x

Cirja MI (2008) Factors affecting the removal of organic micropollutants from wastewater in conventional treatment plants (CTP) and membrane bioreactors (MBR). Rev Environ Sci Biotechnol 7:61–78. https://doi.org/10.1007/s11157-007-9121-8

CLU-IN U (2022) clu-in.org. Retrieved from Contaminated site clean-up information. https://clu-in.org/techfocus/default.focus/sec/Environmental_Fracturing/cat/Overview/

Coates JE (1999) *Geothrix fermentans* gen. nov., sp. Nov., a novel Fe(III)-reducing bacterium from a hydrocarbon-contaminated aquifer. Int J Syst Bacteriol 49(4):1615–1622. https://doi.org/10.1099/00207713-49-4-1615

Coelho CO (2006) The influence of activated carbon surface properties on the adsorption of the herbicide molinate and the bio-regeneration of the adsorbent. J Hazard Mater B138:343–349. https://doi.org/10.1016/j.jhazmat.2006.05.062

Danczak RE (2018) Microbial community cohesion mediates community. Msystems 3(4):e00066-e118. https://doi.org/10.1128/mSystems.00066-18

Das NB (2017) Application of biofilms on remediation of pollutants: an overview. J Microbiol Biotechnol Res 14:783–790

de Jonge RB (1996) Bioregeneration of powdered activated carbon (PAC) loaded with aromatic compounds. Water Res 30:875–882. https://doi.org/10.1016/0043-1354(95)00247-2

Díaz de León G (2021) Impact of anaerobic biofilm formation on sorption characteristics of powdered activated carbon. University of Waterloo, Waterloo. https://uwspace.uwaterloo.ca/bitstream/handle/10012/17164/RochaDiazdeLeon_GriseldaRaquel.pdf?sequence=3

Dolfing JL (2008) Thermodynamic constraints on methanogenic crude oil biodegradation. ISME J 2:442–452

Edwards SJ (2013) Applications of biofilms in bioremediation and biotransformation of persistent organic pollutants, pharmaceuticals/personal care products, and heavy metals. Appl Microbiol Biotechnol 2:9909–9921. https://doi.org/10.1007/s00253-013-5216-z

El Gamal MM-N (2018) Bio-regeneration of activated carbon: a comprehensive review. Separ Purif Technol 197:345–359. https://doi.org/10.1016/j.seppur.2018.01.015

Embree EL-B (2015) Networks of energetic and metabolic interactions. PNAS 112(50):15450–15455. https://doi.org/10.1073/pnas.1506034112

Erickson H (2009) Size and shape of protein molecules at the nanometer level determined by sedimentation, gel filtration, and electron microscopy. Biol Proced Online 11(32):32–51. https://doi.org/10.1007/s12575-009-9008-x

Fan DG (2017) Current state of in situ subsurface remediation by activated carbon-based amendments. J Environ Manag 204:798–803. https://doi.org/10.1016/j.jenvman.2017.02.014

Flemming HW (2010) The biofilm matrix. Nat Rev Microbiol 8(9):623–633. https://doi.org/10.1038/nrmicro2415

Fredrickson JF (2001) Subsurface microbiology and biochemistry. Wiley-Liss Inc., New York

Fundneider TA (2021) Implications of biological activated carbon filters for micropollutant removal in wastewater treatment. Water Res 189:116588. https://doi.org/10.1016/j.watres.2020.116588

García-Delgado CF-S-J (2019) Co-application of activated carbon and compost to contaminated soils: toxic elements mobility and PAH degradation and availability. Int J Environ Sci Technol 16(2):1057–1068. https://doi.org/10.1007/s13762-018-1751-6

Geyer RP (2005) In situ assessment of biodegradation potential using biotraps amended with 13C-labeled benzene or toluene. Environ Sci Technol 39:4983–4989

Gieg LF-C (2014) Syntrophic biodegradation of hydrocarbon contaminants. Curr Opin Biotechnol 27:21–29. https://doi.org/10.1016/j.copbio.2013.09.002

Gonod LV (2006) Spatial distribution of microbial 2,4-dichlorophenoxy acetic acid mineralization fromfield to microhabitat scales. Soil Sci Soc Am J 70:64–71. https://doi.org/10.2136/sssaj2004.0034

Graham EC (2017) Deterministic influences exceed dispersal effects on hydrologically-connected microbiomes. Environ Microbiol 19(4):1552–1567. https://doi.org/10.1111/1462-2920.13720

Greenbank MA (1993) Effects of starting material on activated carbon characteristics and performance. In: Paper presented at WATERTECH Expo '93. Houston, Texas. https://p2infohouse.org/ref/33/32785.pdf

Handley KM (2014) The complete genome sequence for putative H_2- and S-oxidizer *C. sulfuricurvum* sp., assembled de novo from an aquifer-derived metagenome. Environ Microbiol 147:3443–34462

Harris PJF, Liu Z, Suenaga K (2008) Imaging the atomic structure of activated carbon. J Phys Condens Matter 20(36):362201. https://doi.org/10.1088/0953-8984/20/36/362201

Haupt SJ (2019) Migration of chlorinated solvent groundwater plumes with colloidal activated carbon. University of Rhode Island, Kingston. https://digitalcommons.uri.edu/cgi/viewcontent.cgi?article=2481&context=theses

Hayes J (2004) An introduction to isotopic calculations. https://www.whoi.edu/cms/files/jhayes/2005/9/IsoCalcs30Sept04_5183.pdf. Accessed 13 April 2022

Hunkeler DM (2008) A guide for assessing biodegradation and source identification of organic ground water contaminants using compound specific isotope analysis (CSIA). USEPA Office of Research and Development, Ada, Oklahoma. https://cfpub.epa.gov/si/si_public_record_report.cfm?Lab=NRMRL&dirEntryId=202171

IAEA (1993) Reference and intercomparison materials for stable isotopes of light elements. International Atomic Energy Agency, Vienna. https://www-pub.iaea.org/MTCD/publications/PDF/te_825_prn.pdf

ITRC (2020) Optimizing injection strategies and in situ remediation performance. https://ois-isrp-1.itrcweb.org. Accessed 12 Feb 2021

Ji JZ (2020) Methanogenic biodegradation of C9 to C12n-alkanes initiated by Smithella via fumarate addition mechanism. AMB Expr 10(23):956. https://doi.org/10.1186/s13568-020-0956-5

Kharey GSG (2020) Combined use of diagnostic fumarate addition metabolites and genes provides evidence for anaerobic hydrocarbon biodegradation in contaminated groundwater. Microorganisms 8(10):1532. https://doi.org/10.3390/microorganisms8101532

Kim BG (2019) Prokaryotic metabolism and physiology. Cambridge University Press, Cambridge

Kindzierski WG (1992) Activated carbon and synthetic resins as support material for methanogenic phenoldegrading consortia: comparison of surface characteristics and initial colonization. Water Environ Res 64(6):766–775

Kjellerup BA (2013) Application of biofilm covered activated carbon particles as a microbial inoculum delivery system for enhanced bioaugmentation of PCBs in contaminated sediment. In: SERDP Project ER-2135. https://clu-in.org/download/contaminantfocus/pcb/PCBs-Seds-ER-2135-FR-PI.pdf

Klimenko NG (2003a) Bioregeneration of activated carbons by bacterial degraders after adsorption of surfactants from aqueous solutions. Colloids Surf A Physicochem Eng Aspects 230(103):141–158. https://doi.org/10.1016/j.colsurfa.2003.09.021

Klimenko NS (2003b) Bioregeneration of activated carbons by bacterial degraders after adsorption of surfactants from aqueous solutions. Colloids Surf 230(1–3):141–158. https://doi.org/10.1016/j.colsurfa.2003.09.021

Köhler AH (2006) Organic pollutant removal versus toxicity reduction in industrial wastewater treatment: the example of wastewater from fluorescent whitening agent production. Environ Sci Technol 40:3395–3401. https://doi.org/10.1021/es060555f

Kolasinski KW (2019) Surface science: foundations of catalysis and nanoscience, 4th edn. Wiley, Hoboken. https://www.perlego.com/book/1284212/surface-science-pdf

Krüger US (2019) Bacterial dispersers along preferential flow paths of a clay till depth profile. Appl Environ Microbiol 85(6):e02658-e2718. https://doi.org/10.1128/AEM.02658-18

Kupryianchyk DR (2013) In situ treatment with activated carbon reduces bioaccumulation in aquatic food chains. Environ Sci Technol 11:4563–4571. https://doi.org/10.1021/es305265x

Laban NA-F (2015) Draft genome sequence of uncultivated toluene-degrading desulfobulbaceae bacterium Tol-SR, obtained by stable isotope probing using [13C6]toluene. Microbiol Resour Announc 3(1):1–2. https://doi.org/10.1128/genomeA.01423-14

Leglize PA (2008) Adsorption of phenanthrene on activated carbon increases mineralization rate by specific bacteria. J Hazard Mater 151(2–3):339–347. https://doi.org/10.1016/j.jhazmat.2007.05.089

Lhotský OK (2021) The effects of hydraulic/pneumatic fracturing-enhanced remediation (FRAC-IN) at a site contaminated by chlorinated ethenes: a case study. J Hazard Mater 417:125883. https://doi.org/10.1016/j.jhazmat.2021.125883

Li AY (1983) Availability of sorbed substrate for microbial degradation on granular activated carbon. J Water Pollut Control Feder 12:392–399

Li LL (2011) Surface modification of coconut shell based activated carbon for the improvement of hydrophobic VOC removal. J Hazard Mater 192(2):683–690. https://doi.org/10.1016/j.jhazmat.2011.05.069

Liang CC (2007) Modeling the behaviors of adsorption and biodegradation in biological activated carbon filters. Water Resour 41:3241–3250

Liang YZ (2008) Porous biocarrier-enhanced biodegradation of crude oil contaminated soil. Int Biodeter Biodegrad 63:80–87. https://doi.org/10.1016/j.ibiod.2008.07.005

Lillo-Ródenas MC-A-S (2005) Behaviour of activated carbons with different pore size distributions and surface oxygen groups for benzene and toluene adsorption at low concentrations. Carbon 43(8):1758–1776. https://doi.org/10.1016/j.carbon.2005.02.023

Liu FR-E (2012) Promoting direct interspecies electron transfer with activated carbon. Energy Environ Sci 47:8982. https://doi.org/10.1039/C2EE22459C

Lovley D (2017) Syntrophy goes electric: direct interspecies electron transfer. Annu Rev Microbiol 117:643–664. https://doi.org/10.1146/annurev-micro-030117-020420

Lu ZS (2020) Effect of granular activated carbon pore-size distribution on biological activated carbon filter performance. Water Res 177(15):115768. https://doi.org/10.1016/j.watres.2020.115768

Luckner LS (1991) Migration process in soil and groundwater zone. Bundesrepublik Deutschland, Leipzig

Ma XZ (2019) Adsorption of volatile organic compounds at medium-high temperature conditions by activated carbons. Energy Fuels 34(3):3679–3690. https://doi.org/10.1021/acs.energyfuels.9b03292

Maamar SA-C-A (2015) Groundwater isolation governs chemistry and microbial community structure along hydrologic flowpaths. Front Microbiol 6:13. https://doi.org/10.3389/fmicb.2015.01457

Mackenstock RM (2004) Stable isotope fractionation analysis as a tool to monitor biodegradation in contaminated acquifers. Contam Hydrol 75:215–255. https://doi.org/10.1016/j.jconhyd.2004.06.003

Mancini SA-C (2003) Carbon and hydrogen isotopic fractionation during anaerobic biodegradation of benzene. Appl Environ Microbiol 69(1):191–198. https://doi.org/10.1128/AEM.69.1.191-198.2003

Mangrich AS (2015) Improving the water holding capacity of soils of northeast Brazil by biochar augmentation. In: Satinder Ahuja JB (ed) Water challenges and solutions on a global scale (ACS symposium series), 1st edn. American Chemical Society, New York, pp 339–354

Mangse GW (2020) Carbon mass balance model to investigate biochar and activated carbon amendment effects on the biodegradation of stable-isotope labeled toluene in gravelly sand. Environ Adv 2:100016. https://doi.org/10.1016/j.envadv.2020.100016

Marchal GS (2013) Impact of activated carbon, biochar and compost on the desorption and mineralization of phenanthrene in soil. Environ Pollut 181:200–210. https://doi.org/10.1016/j.envpol.2013.06.026

Marozava SR (2014) Physiology of *G. metallireducens* under excess and limitation of electron donors. Part I. Batch cultivation with excess of carbon sources. Syst Appl Microbiol 37(4):277–286. https://doi.org/10.1016/j.syapm.2014.02.004

Massol-Deyá AA (1995) Channel structures in aerobic biofilms of fixed-film reactors treating contaminated groundwater. Appl Environ Microbiol 6(12):769–777. https://doi.org/10.1128/aem.61.2.769-777.1995

McCormick (2010) McCormick and baxter superfund site stockton: study report. Study Report Task Order No. 0018

McGregor R (2020) Distribution of colloidal and powdered activated carbon for the in situ treatment of groundwater. J Water Resour Protect 12(12):1001–1018. https://doi.org/10.4236/jwarp.2020.1212060

McNamara JF (2018) Comparison of activated carbons for removal of perfluorinated compounds from drinking water. JAWWA 110:E2–E14. https://doi.org/10.5942/jawwa.2018.110.0003

Meckenstock RU (1999) 13C/12C isotope fractionation of aromatic hydrocarbons during microbial degradation. Environ Microbiol 1(5):409–414. https://doi.org/10.1046/j.1462-2920.1999.00050.x

Menendez Diaz JA-G (2006) Types of carbon adsorbents and their production. Elsevier, Amsterdam

Meynet PH (2012) Effect of activated carbon amendment on bacterial community structure and functions in a PAH impacted urban soil. Environ Sci Technol 46:5057–5066. https://doi.org/10.1021/es2043905

Morsen ARH (1987) Degradation of phenol by mixed culture of *Pseudomonas putida* and *Cryptococcus elinovii* adsorbed on activated carbon. Appl Microbial Biotechnol 26:283–288. https://doi.org/10.1007/BF00286325

Morsen AR (1990) Degradation of phenol by a defined mixed culture immobilized by adsorption on activated carbon and sintered glass. Appl Microbial Biotechnol 33:206–212. https://doi.org/10.1007/BF00176526

Murdoch L (1995) Forms of hydraulic fractures created during a field test in fine-grained glacial drift. Q J Eng Geol 28:23–35. https://doi.org/10.1144/GSL.QJEGH.1995.028.P1.03

Nath KB (2011a) Bioregeneration of spent activated carbon: effect of physico-chemcial parameters. J Sci Ind Res 70:487–492

Nath KB (2011b) Microbial regeneration of spent activated carbon dispersed with organic contaminants: mechanism, efficiency, and kinetic models. Environ Sci Pollut Res Int 18(4):534–546. https://doi.org/10.1007/s11356-010-0426-8

Noland S (2002) United States Patent No. 7,787,034 B2

Or DS (2007) Physical constraints affecting bacterial habitats and activity in unsaturated porous media: a review. Adv Water Resour 30:1505–1527. https://doi.org/10.1016/j.advwatres.2006.05.025

Pagnozzi G (2020) Evaluating the influence of capping materials on composition and biodegradation activity of benthic microbial communities: implications for designing bioreactive sediment caps. Texas Tech University, Civil Engineering, Texas Tech, Lubbock

Pagnozzi GC (2021) Powdered activated carbon (PAC) amendment enhances naphthalene biodegradation under strictly sulfate-reducing conditions. Environ Pollut 268:115641. https://doi.org/10.1016/j.envpol.2020.115641

Peacock AD-J (2004) Utilization of microbial biofilms as monitors of bioremediation. Microb Ecol 47:284–292

Perrotti AR (1974) Factors involved with biological regeneration of activated carbon. Am Inst Chem Eng Symp Ser 144:316–325

Piai LD (2019) Diffusion of hydrophilic organic micropollutants in granular activated. Water Res 162:518–527. https://doi.org/10.1016/j.watres.2019.06.012

Piai LB (2020) Biodegradation and adsorption of micropollutants by biological activated carbon from a drinking water production plant. J Hazard Mater 388:122028. https://doi.org/10.1016/j.jhazmat.2020.122028

Piai LV (2021) Melamine degradation to bioregenerate granular activated carbon. J Hazard Mater 414:125503. https://doi.org/10.1016/j.jhazmat.2021.125503

Piai LL (2022) Prolonged lifetime of biological activated carbon filters through enhanced biodegradation of melamine. J Hazard Mater 422:126840. https://doi.org/10.1016/j.jhazmat.2021.126840

Ran JS (2018) Remediation of polychlorinated biphenyls (PCBs) in contaminated soils and sediment: state of knowledge and perspectives. Front Environ Sci 14:79. https://doi.org/10.3389/fenvs.2018.00079

Rattier MR (2012) Organic micropollutant removal by biological activated carbon filtration: a review. Urban Water Security Research Alliance, Queensland

Regenesis (2022) regenesis.com: https://regenesis.com/wp-content/uploads/2019/02/brochure_4.1.pdf

Rhodes AH (2010) Impact of activated charcoal on the mineralisation of 14C-phenanthrene in soils. Chemosphere 79(4):463–469. https://doi.org/10.1016/j.chemosphere.2010.01.032

Rotaru AC-W (2018) Conductive particles enable syntrophic acetate oxidation between geobacter and methanosarcina from coastal sediments. Mbio 9(3):e00226-e318. https://doi.org/10.1128/mBio.00226-18

Ruthven D (1984) Principals of adsorption and adsorption processes. John Wiley & Sons, New York

Santamarina VR-L (2006) Mechanical limits to microbial activity in deep sediments. Geochem Geophys Geosyst 7:1525–2027. https://doi.org/10.1029/2006GC001355

Schüth CT (2003) Carbon and hydrogen isotope effects during sorption of organic contaminants on carbonaceous materials. J Contam Hydrol 64(3–4):269–281. https://doi.org/10.1016/S0169-7722(02)00216-4

Semenyuk NN (2014) Effect of activated charcoal on bioremediation of diesel fuel-contaminated soil. Microbiology 83:589–598. https://doi.org/10.1134/S0026261714050221

Siegrist RL (1998) X-231A demonstration of in situ remediation of DNAPL compounds in low permeability media by soil fracturing with thermally enhanced mass recovery or reactive barrier destruction. Oak Ridge National Laboratory and Collaborators, Oak Ridge. https://clu-in.org/download/techfocus/fracturing/X231A-3445604441067.pdf

Slater GA-K (2000) Carbon isotope effects resulting from equilibrium sorption of dissolved VOCs. Anal Chem 72(22):5669–5672. https://doi.org/10.1021/ac000691h

Smith HJ (2018) Impact of hydrologic boundaries on microbial planktonic and biofilm communities in shallow terrestrial subsurface environments. FEMS Microbiol Ecol 94(12):191. https://doi.org/10.1093/femsec/fiy191

Smolin SK (2020) New approach for the assessment of the contribution of adsorption, biodegradation and self-bioregeneration in the dynamic process of biologically active carbon functioning. Chemosphere 248:126022. https://doi.org/10.1016/j.chemosphere.2020.126022

Sorenson KN (2019) Use of permeability enhancement technology for enhanced in situ remediation of low-permeability media. Department of Defense Environmental Security Technology Certification Program (ESTCP), Alexandria, VA. file:///C:/Users/winne/Downloads/ER-201430%20Guidance%20Document%20(2).pdf

Sublette KS (1982) A review of the mechanism of powdered activated carbon enhancement of activated sludge treatment. Water Res 16(7):1075–1082. https://doi.org/10.1016/0043-1354(82)90122-1

Summers ZF (2010) Direct exchange of electrons within aggregates of an evolved syntrophic coculture of anaerobic bacteria. Science 330(6009), pp. 1413–1415. https://www.science.org/doi/10.1126/science.1196526

Thies JE (2012) In biochar for environmental management. Routledge, London. https://doi.org/10.4324/9781849770552

Thomas WJ (1998) Absorption technology and design. Reed Educational and Professional Publishing Ltd., Oxford

Weber W, Pirbazari M, Melson G (1978) Biological growth on activated carbon: an investigation by scanning electron microscopy. Environ Sci Technol 12(7):817–819. https://doi.org/10.1021/es60143a005

Weiss TH (1995) Effect of bacterial cell shape on transport of bacteria in porous media. Environ Sci Technol 29(7):1737–1740. https://doi.org/10.1021/es00007a007

Williams N, Hyland A, Mitchener R, Sublette K, Key K, Davis G et al (2013) Demonstrating the in situ biodegradation potential of phenol using Bio-Sep® Bio-Traps® and stable isotope probing. Remediation 23(1):7–22. https://doi.org/10.1002/rem.21335

Xiaojian ZZ (1991) Simple combination of biodegradation and carbon adsorption—the mechanism of the biological activated carbon process. Water Res 25(2):165–172. https://doi.org/10.1016/0043-1354(91)90025-L

Yee MO-W (2019) Extracellular electron uptake by two methanosarcina species. Front Energy Res 29:19. https://doi.org/10.3389/fenrg.2019.00029

Yu YL (2021) Influence of pore structure on biologically activated carbon performance and biofilm microbial characteristics. Front Environ Sci Eng 15(6):1–13. https://doi.org/10.1007/s11783-021-1419-1

Zamulina IP (2020) The effect of granular activated carbon on the physical properties of soils at copper contamination. In: E3S web of conferences. EDP Sciences, Rostovon-Don, pp 1–6. https://doi.org/10.1051/e3sconf/202017509003

Zango ZS (2020) An overview and evaluation of highly porous adsorbent materials for polycyclic aromatic hydrocarbons and phenols removal from wastewater. Water 12(10):2921. https://doi.org/10.3390/w12102921

Zapata Acosta KC-M (2019) Immobilization of *P. stutzeri* on activated carbons for degradation of hydrocarbons from oil-in-saltwater emulsions. Nanomaterials 9(4):500. https://doi.org/10.3390/nano9040500

Zhang WD (2013) Biological activated carbon treatment for removing BTEX from groundwater. J Environ Eng 139(10):1246–1254. https://doi.org/10.1061/(ASCE)EE.1943-7870.0000731

Żur JW (2016) Metabolic responses of bacterial cells to immobilization. Molecules 21:958. https://doi.org/10.3390/molecules21070958